T.R.
ONDOKUZ MAYIS UNIVERSITY
INSTITUTE OF GRADUATE STUDIES
DEPARTMENT OF SOIL SCIENCE AND PLANT NUTRITION

SOIL FERTILITY EVALUATION THROUGH REMOTE SENSING AND *IN-SITU* ANALYSES OF TEST WHEAT PLANTS

Master's Thesis

Endalkachew Abebe KEBEDE

Supervisor

Assoc. Prof. Dr. Bojin BOJINOV

II. Supervisor

Prof. Dr. Orhan DENGIZ

SAMSUN

2022

T.R.
ONDOKUZ MAYIS UNIVERSITY
INSTITUTE OF GRADUATE STUDIES
DEPARTMENT OF SOIL SCIENCE AND PLANT NUTRITION

SOIL FERTILITY EVALUATION THROUGH REMOTE SENSING AND *IN-SITU* ANALYSES OF TEST WHEAT PLANTS

Master's Thesis

Endalkachew Abebe KEBEDE

Supervisor

Assoc. Prof. Dr. Bojin BOJINOV

II. Supervisor

Prof. Dr. Orhan DENGIZ

This thesis was supported by the European Union project of Erasmus Mundus Joint Master Degree in Soil Science (emiSS) with project number 610528-EPP-1-2019-1-TR-EPPKA1-JMD-MOB.

SAMSUN

2022

ACCEPTANCE AND APPROVAL OF THESIS

The study entitled "**SOIL FERTILITY EVALUATION THROUGH REMOTE SENSING AND IN SITU ANALYSES OF TEST WHEAT PLANTS**" prepared by **Endalkachew Abebe KEBEDE,** and supervised by **Assoc. Prof. Bojin BOJINOV and Prof. Dr. Orhan DENGIZ ,** was found successful and unanimously accepted by committee members as Master thesis, following the examination on the date 06/07/ 2022.

	Title Name SURNAME University Department/Art	**Signature**	**Final Decision**
Chairman	Assoc. Prof. Dr. Bojin BOJINOV Agricultural University-Plovdiv Department of Plant Physıology, Biochemıstry and Genetıcs		☒ Accept ☐ Reject
Member	Prof. Dr. Orhan DENGIZ Ondokuz Mayıs University Department of Soil Science and Plant Nutrition		☒ Accept ☐ Reject
Member	Prof. Dr. Andon Vasilev ANDONOV Agricultural University-Plovdiv Department of Plant Physıology, Biochemıstry and Genetıcs		☒ Accept ☐ Reject
Member	Prof. Dr. Coşkun GÜLSER Ondokuz Mayıs University Department of Soil Science and Plant Nutrition		☒ Accept ☐ Reject
Member	Prof. Dr. Rıdvan KIZILKAYA Ondokuz Mayıs University Department of Soil Science and Plant Nutrition		☒ Accept ☐ Reject

This thesis has been approved by the committee members that already stated above and determined by the Institute Executive Board.

APPOVAL

... / ... / ...

Prof. Dr. Ali BOLAT

Head of Institute of Graduate Studies

DECLARATION OF COMPLIANCE WITH SCIENTIFIC ETHIC

I hereby declare and undertake that I complied with scientific ethics and academic rules in all stages of my Master's Thesis, that I have referred to each quotation that I use directly or indirectly in the study, and that the works I have used consist of those shown in the sources, that it was written in accordance with the institute writing guide and that the situations stated in the article 3, section 9 of the Regulation for TÜBİTAK Research and Publication Ethics Board were not violated.

Is Ethics Committee Necessary?

Yes ☐ (If it is necessary, please add appendices.)

No ☒

16/06/2022

Endalkachew Abebe Kebede

DECLARATION OF THE THESIS STUDY ORIGINALITY REPORT

Thesis Title: SOIL FERTILITY EVALUATION THROUGH REMOTE SENSING AND IN-SITU ANALYSES OF TEST WHEAT PLANTS

As a result of the originality report taken by me from the plagiarism detection program on 13 /06 /2022 for the thesis titled above;

Similarity ratio : % 13

Single resource rate :% 3 has been released.

16/06/2022

Prof. Dr. Orhan DENGIZ

ÖZET

TEST BUĞDAY TESISLERININ UZAKTAN ALGILAMA VE YERINDE ANALIZLERI ILE TOPRAK VERIMLILIĞI DEĞERLENDIRMESI

Tez Yazarının Endalkachew Abebe KEBEDE
Ondokuz Mayıs Üniversitesi
Lisansüstü Eğitim Enstitüsü
Toprak Bilimi ve Bitki Besleme Bölümü
Yüksek Lisans, Temmuz/2022
Danışman I: Doç. Dr. Bojin BOJINOV

Uzaktan algılama, bitkilerin ve toprakların elektromanyetik spektrum içindeki spektral tepkilerini kullanarak bitkilerin biyofiziksel özelliklerini değerlendirme ve izlemede potansiyel bir uygulamaya sahiptir. Ancak, yalnızca birkaç rapor, farklı uzaktan algılama sensörlerinin performansını yerinde alan spektral ölçümüyle karşılaştırır. Mevcut çalışma, Ovcha Mogila köyünde bulunan bir çalışma çiftliğinde Buğday mahsulünün biyofiziksel özelliklerini tahmin etmede açık veri kaynaklı uydu görüntülerinin (Sentinel 2 ve Landsat 9) potansiyel uygulamalarını değerlendirdi. Açık veri kaynaklarından Aralık 2021 – Nisan 2022 dönemi için %10'dan daha az bulut örtüsüne sahip Landsat 9 (30 m çözünürlük) ve Sentinel-2 (10 m çözünürlük) uydu görüntüleri alınmıştır. İnsansız Hava Aracı (İHA)) bitki yapraklarının spektral tepkisini yakalamak için kullanılmıştır. Ek olarak, SpectraVue 710s Yaprak Spektrometresi, Nisan ayında aynı tarla içinde beş farklı lokasyonda mahsulün spektral tepkisini ölçmek için kullanıldı. En yaygın on bitki indeksi seçilmiş ve kullanılan uzaktan algılama araçlarının yansıma dalga boyu aralığına göre hesaplanmıştır. Toprak örnekleri, çiftlik arazisi içinde sekiz farklı yerden toplanmıştır. Toprağın farklı fizikokimyasal özellikleri (pH, doku, N, P_2O_5 ve K_2O) laboratuvarda analiz edilmiştir. UAV ve Yaprak Spektrometresinden alınan daha iyi çözünürlüklü görüntüler, uydu görüntülerini doğrulamak için kullanılmıştır. Farklı sensörlerin performansı, ölçülen yaprak spektral tepkisine ve beş örnekleme noktası kullanılarak çıkarılan bitki örtüsü endekslerine dayalı olarak karşılaştırılmıştır. Sentinel 2 ve Landsat 9 VI'nın performansını karşılaştırmak için saptama katsayısı (R^2) ve Ortalama Kare Hatası (RMSE) ve corr ve heatmap python kütüphaneleri kullanılarak hazırlanan korelasyon (r) matrisi ile bir dağılım grafiği kullanılmıştır. dron. Toprak analizi, çalışma çiftliğinin hafif alkali olduğunu ortaya çıkardı (8,4 ila 8,52). Çalışma çiftliğinin toprak dokusu ağırlıklı olarak Kil ve Kil-Tındır. Bitki örtüsü indeksleri (VI), bitkinin büyümesiyle doğrusal olarak artmıştır. Hem dağılım grafiği hem de korelasyon matrisi, Sentinel 2 bitki örtüsü endekslerinin, Landsat 9'a kıyasla Bueto drone'nun bitki örtüsü endeksleri ile nispeten daha iyi bir korelasyona sahip olduğunu gösterdi. Landsat 9 bitki örtüsü endeksleri, yaprak spektrometresi ile bir şekilde daha iyi hizalanır. Genel olarak, Sentinel 2, Landsat 9'dan daha iyi bir performans gösterdi. Mevcut çalışmanın kalitesini iyileştirmek için yeterli alan spektral örnekleme ve tekrarlanan UAV görüntüleme ile daha fazla çalışma gereklidir.

Anahtar Kelimeler: Sentinel 2, Landsat 9, İHA, Yaprak Spektrometresi

ABSTRACT

SOIL FERTILITY EVALUATION THROUGH REMOTE SENSING AND IN-SITU ANALYSES OF TEST WHEAT PLANTS

Endalkachew Abebe KEBEDE
Ondokuz Mayıs University
Institute of Graduate Studies
Department of Soil Science and Plant Nutrition
Master, June/2022
Supervisor: Assoc. Prof. Dr. Bojin BOJINOV

Remote sensing has a potential application in assessing and monitoring the plants' biophysical properties using the spectral responses of plants and soils within the electromagnetic spectrum. However, only a few reports compare the performance of different remote sensing sensors against *in-situ* field spectral measurement. The current study assessed the potential applications of open data source satellite images (Sentinel 2 and Landsat 9) in estimating the biophysical properties of the wheat crop on a study farm found in the village of Ovcha Mogila. A Landsat 9 (30 m resolution) and Sentinel-2 (10 m resolution) satellite images with less than 10% cloud cover have been extracted from the open data sources for the period of December 2021 to April 2022. An Unmanned Aerial Vehicle (UAV) has been used to capture the spectral response of plant leaves. In addition, SpectraVue 710s Leaf Spectrometer was used to measure the spectral response of the crop in April at five different locations within the same field. The ten most common vegetation indices have been selected and calculated based on the reflectance wavelength range of remote sensing tools used. The soil samples have been collected in eight different locations within the farm plot. The different physicochemical properties of the soil (pH, texture, N, P_2O_5, and K_2O) have been analyzed in the laboratory. The finer resolution images from the UAV and the Leaf Spectrometer have been used to validate the satellite images. The performance of different sensors has been compared based on the measured leaf spectral response and the extracted vegetation indices using the five sampling points. A scatter plot with the coefficient of determination (R^2) and Root Mean Square Error (RMSE) and the correlation (r) matrix prepared using the corr and heatmap python libraries have been used for comparing the performance of Sentinel 2 and Landsat 9 VIs compared to the drone and SpectraVue 710s spectrophotometer. The soil analysis revealed the study farm plot is slightly alkaline (8.4 to 8.52). The soil texture of the study farm is dominantly Clay and Clay Loam. The vegetation indices (VIs) increased linearly with the growth of the plant. Both the scatter plot and the correlation matrix showed that Sentinel 2 vegetation indices have a relatively better correlation with the vegetation indices of the Buteo drone compared to the Landsat 9. The Landsat 9 vegetation indices somewhat align better with the leaf spectrometer. Generally, the Sentinel 2 showed a better performance than the Landsat 9. Further study with enough field spectral sampling and repeated UAV imaging is required to improve the quality of the current study.

Keywords: Sentinel 2, Landsat 9, UAV, Leaf Spectrometer

ACKNOWLEDGMENTS

I am deeply indebted to the Erasmus Mundus Joint Master Degree in Soil Science (emiss) Program for providing the scholarship to pursue my Masters's Degree.

I also would like to express my sincere gratitude to my supervisors, Assoc. Prof. Dr. Bojin Bojinov, Prof. Dr. Andon Vasilev Andonov, and Prof. Dr. Orhan Dengiz for their endless support, continuous encouragement, and professional guidance during the whole process. I am honored to do my MSc thesis under their supervision.

Finally, I would like to thank my classmates for their support during my study.

Endalkachew Kebede

CONTENTS

SYMBOLS AND ABBREVATIONS

CHLG	:Chloropropyl index Green
CHLR	:Chloropropyl index Red
EVI	:Enhanced Vegetation Index
GNDVI	:Green Normalized Difference Vegetation Index
MCARI	:Modified Chlorophyll Absorption Ratio Index
NDVI	: Normalized Difference Vegetation Index
NDMI	: Normalized Difference Moisture Index
MSI	: Multi Spectral Instrument
OLI	: Operational Land Imager
r	: Pearson correlation coefficient
R^2	: Coefficient of determination
RMSE	: Root Mean Square Error
RS	: Remote Sensing
SR	: Simple Ratio
SAVI	: Soil Adjusted Vegetation Index
SIPI	: Structure Insensitive Pigment Index
UAV	: Unammned Aerial Vehicle

FIGURES LEGENDS

TABLES LEGENDS

1. INTRODUCTION

Agriculture has evolved since its inception for over thousands of years. Remarkably, there has been a significant advancement in agricultural practices following the industrial revolution since the 1700s (Thrall et al., 2010). The introduction of tillage machinery, improved varieties, organic soil fertility amendments, inorganic fertilizers, and other technologies have substantially improved agricultural production and promoted large-scale farming (Liaghat & Balasundram, 2010)

The global population has been rising drastically since the Holocene epoch. The current global population is estimated to be 7.5 billion, and it is projected to peak at 10 billion by the end of 2050 (Cervantes-Godoy et al., 2014). Advanced agricultural practice is crucial to meet the expanding food and fiber demand of the global community and promote sustainable development (Ennouri et al., 2021; Liaghat & Balasundram, 2010)

Despite the benefit of different sectors by technological advancements, the agriculture sector is limitedly exploiting it (World Economic Forum, 2021). Adequate application of agricultural practices is highly dependent on the information available to the decision-makers. The availability of updated weather data (precipitation and temperature, flood/drought), physically based and remotely sensed crop data, updated market information, and the latest agricultural approaches has been validated to substantially improve production and productivity (Darnhofer et al., 2010).

Remote sensing (RS) is a method of capturing, storing, and analyzing the information gathered from a distance without getting in touch with the object (Ray, 2016). RS allows the analysis of a multispectral image that is useful for identifying and characterizing different Earth features, including soil, vegetation, and water. This technology allows for monitoring the farming practices, identifying potential plant stress, and selecting and applying different management approaches to optimize the yield (Moussaid et al., 2021). Remote sensing has become a new trend in the current agricultural research (Moussaid et al., 2021; Ray, 2016).

Although the RS has been applied in different sectors successfully, its application in agriculture is still limited (Tenkorang & Lowenberg-DeBoer, 2008). The potential application of remote sensing in assessing the soil and cop condition with few input data and acceptable accuracy has been discussed by several researchers (Aguiar et al., 2011; Arvor et al., 2011; Bégué et al., 2019; Kingra et al., 2016; Ray, 2016; Shanmugapriya et al., 2019; Sullivan et al.,

2008). RS also has an essential application for estimating nutrient and soil moisture in the absence of physical measurement at acceptable accuracy (Casanova et al., 2006; Nellis et al., 2009; Shanmugapriya et al., 2019). The role of RS in agriculture is also extended to assessing crop health, identifying weeds, estimating crop yield, and promoting precise farming (Lorenzen & Jensen, 1989; West et al., 2003).

Several studies focused on a single remote sensing approach, either using satellite images (Aguiar et al., 2011; Arvor et al., 2011; Bégué et al., 2019; Léna Maatoug, Damien Arvor, Margareth Simões, 2012; Ozdogan, 2010; Sullivan et al., 2008) or UAV (Francesconi et al., 2021; Han et al., 2021). Most of these studies don't compare the accuracy of RS against field data. Only a few reports compared the RS predictions against the *in-situ* field measurement (Croft et al., 2020; Darvishzadeh et al., 2019; Ulfa et al., 2022).

This study presented herein was conducted in a farm field found in the small city of Ovcha Mogila, located in the central part of the Danube hilly lowland about 20 km south of the town Svishtov (Wikipedia, 2022). Several studies have evaluated the application of RS in Bulgarian agriculture. Most RS studies in Bulgaria focus on urban and agricultural land management (Dimitrov et al., 2021; Kolev & Kozelov, 2015; Stoyanov et al., 2019). Gikov et al. (2019) demonstrated the Sentinel 2 satellite imagery application for preparing a crop-type map of targeted small regions in Bulgaria. Dimitrov et al. (2021) extended this work by preparing the crop mapping at a national level. However, scientific studies about comparing the accuracy of satellite images and Unmanned Aerial Vehicle (UAV)-based vegetation indices on estimating a crop's biophysical properties against the field measurement are still incomplete in the study area.

The general objective of this study was to assess the biophysical properties of the crop using a remote sensing approach and *in-situ* field measurements and analysis. The current study is novel to evaluate the potential application of the remote sensing approach to assess soil and crop condition compared to the *in-situ* field measurement. It contrasts spatial resolution and estimation accuracy of satellite images from open data sources and digital images from a UAV. The different biophysical characteristics of the crop have been assessed by developing vegetation indices. The accuracy of selected vegetation indices was validated against the field measurement.

Objectives of the Study

The general objective of this study was to assess the biophysical properties of the crop using a remote sensing approach and *in-situ* field measurements and analysis.

The study has the following specific objectives. These are:

1. To assess the biophysical properties of the test wheat crop based on satellite and UAV digital image analysis techniques.
2. To evaluate the crop condition by measuring *in-situ* the spectral transmission, absorption, and reflection of light and applying vegetation indices.
3. To validate the performance of RS in estimating biophysical properties of the crop at acceptable accuracy against the field measurement.

2. LITERATURE REVIEW

2.1. Remote Sensing

RS is the method of data acquisition about objects or areas without contacting them at a remote location. It is a tool that provides a synoptic observation of Earth's features (Moussaid et al., 2021). The remote sensing approach is based on collecting data from a broad electromagnetic spectrum – a wavelength range of electromagnetic radiation that ranges from visible to infrared and microwave. It is based on the knowledge that each feature has a unique response at a different wavelength range. This response allows identifying the targeted features, as shown in Figure 2.1 (Shanmugapriya et al., 2019).

The maximum absorption in plants is found within the spectral regions of blue (400-500nm) and red (660-680nm). A healthy plant looks green as it absorbs more blue and red light while reflecting green and infrared (Shanmugapriya et al., 2019).

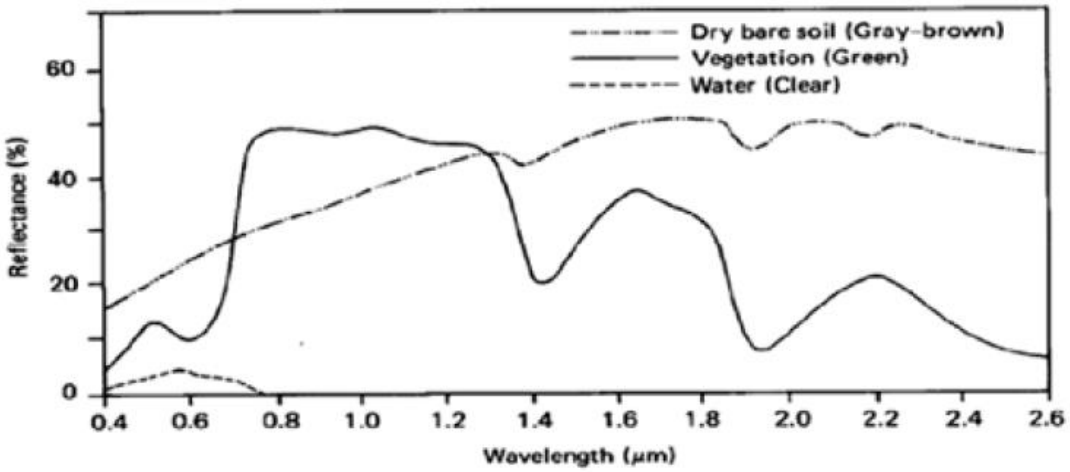

Figure 2.1. The response of different Earth features to different wavelength regions (Kingra et al., 2016)

Recent advancements in RS with improved data acquisition, processing, and interpretation of ground-based, airborne, and satellite data present an opportunity to monitor different agricultural practices at a finer resolution (Liaghat & Balasundram, 2010). The main advantage of remote sensing over physical measurement and analysis is its cost-effectiveness and collection of the necessary data with many repetitions without damaging agricultural soils or crops during sampling (Kingra et al., 2016; Shanmugapriya et al., 2019).

Satellite observation of the Earth's features is vital for a better understanding of the natural processes. Different satellite-based observation data are available that vary in the type of sensor, spectral, temporal, and spatial resolution (Oza et al., 2008). The United States

Geological Survey (USGS) Landsat and the European Union Copernicus program Sentinel satellites have been among the most successful ones (Colin et al., 2012; I. Yang & Acharya, 2015).

The Landsat program started in the early 1970s to provide a global synoptic observation of the Earth's features at a moderate resolution to monitor anthropogenic-induced changes (USGS, 2013). The USGS's Landsat data has been one of the most reliable data sources for monitoring and mapping the Earth's features over the last five decades (Hansen & Loveland, 2012; I. Yang & Acharya, 2015). Of the nine Landsat satellites, the Landsat 5 started producing images in the 1980s and operated successfully beyond expectations before it stopped delivering images from its primary sensor in 2011. The Landsat 6 could not reach orbit. The Landsat 7 has an image quality problem with striping the missing data (USGS, 2013). The Landsat 8 satellite was launched in 2013 with a clearer view feature and better brightness and color sensitivity than previous Landsat satellites (I. Yang & Acharya, 2015).

The Landsat 9 has a swath width of 185 km and a sensing repetition cycle of 16 days. It has two main instruments: Operational Land Imager (OLI-2) and Thermal Infrared Sensor (TIRS-2), which produce continuous images consisting of nine spectral bands. The OLI-2 collects imagery data in visible, Near Infrared (NIR) wavelength, shortwave infrared at 30 m spatial resolution, and the panchromatic band at 15 m spatial resolution (Table 2.1). The TIRS-2 instrument gathers the thermal infrared bands at 100 m spatial resolution (USGS, 2021).

The European Commission Copernicus program has launched three satellites (Sentinel 1, 2, and 3A) to provide free imagery for the global scientific community (Drusch et al., 2012; Malenovský et al., 2012). The Sentinel-1 is designed to produce continuous data within the microwave wavelength range for the next two decades. Sentinel-2 and 3 collect images within the optical wavelength range (Berger et al., 2012).

Sentinel-2A sensor was launched in 2015, which has a swath width of 290 km and a sensing repetition cycle of 10 days to produce multispectral images with 13 bands with different spatial resolutions. The sensor has a spatial resolution of 10 m, 20 m, and 60 m. Four visible and NIR bands have 10 m spatial resolutions. Six red edges and Shortwave Infrared (SWIR) bands have a 20 m spatial resolution, and three atmospheric corrections bands have a 60 m resolution (Drusch et al., 2012).

Table 2.1. The wavelength range and spatial resolution of Sentinel-2 and Landsat 9 satellites used in the study

Sentinel-2			Landsat 9		
Band	Resolution (m)	Wavelength range (nm)	Band	Resolution (m)	Wavelength range (nm)
Band 2(blue)	10	458–523	Band 2(blue)	30	452–512
Band 3(green)	10	543–578	Band 3(green)	30	533–590
Band 4 (red)	10	650–680	Band 4 (red)	30	636–673
Band 8 (NIR)	10	785–900	Band 5 (NIR)	30	851–879
Band 8A (NIR)	20	855–875			
B11(SWIR-1)	20	1565–1655	Band 6	30	1566–1651
B12(SWIR-2)	20	2100–2280	Band 7	30	2107–2294

The other remote sensing approach commonly used to monitor agricultural practices is the Unmanned Aerial Vehicle (UAV). UAVs, also called drones, have become the new trend in agricultural research. UAVs can have attached a multispectral sensor to produce a real-time observation at a specific spatial extent. Besides, compared to the satellites, the UAV sensors have exceptionally finer spatial (0.2 m) and temporal resolutions, enabling precise and cost-effective data collection (Ndlovu et al., 2021).

2.2 Remote Sensing in Agriculture

The previous research trend of Remote Sensing was focused on satellite images to prepare land use/land cover classification maps. The Land cover classification maps indicate the area of the vegetation or cropland. The current remote sensing studies are focused mainly on plant and soil biological and physical properties (Shanmugapriya et al., 2019).

As depicted in Figure 2.2, studies about RS applications in agriculture have increased significantly over the last two decades. This implied that there had been a significant technological advancement, including spatial, temporal, and spectral resolutions of sensors, Unmanned Aerial Vehicles (UAV), and the progressive growth of cloud computing and machine learning techniques applications. UAV-based remote sensing showed slow progress until 2015 and then a distinct increasing trend between 2015 and 2019. Between these four years, the number of studies based on UAVs increased by at least 23%. Besides, the studies based on satellite and aerial images showed an increasing trend. This is due to the improved accessibility of satellite images through open data sources (USGS and Sentinel) and cloud computing platforms (Google Earth Engine). Currently, the number of studies about remote sensing applications in agriculture is roughly 20 times more than in the 2000s (Khanal et al., 2020).

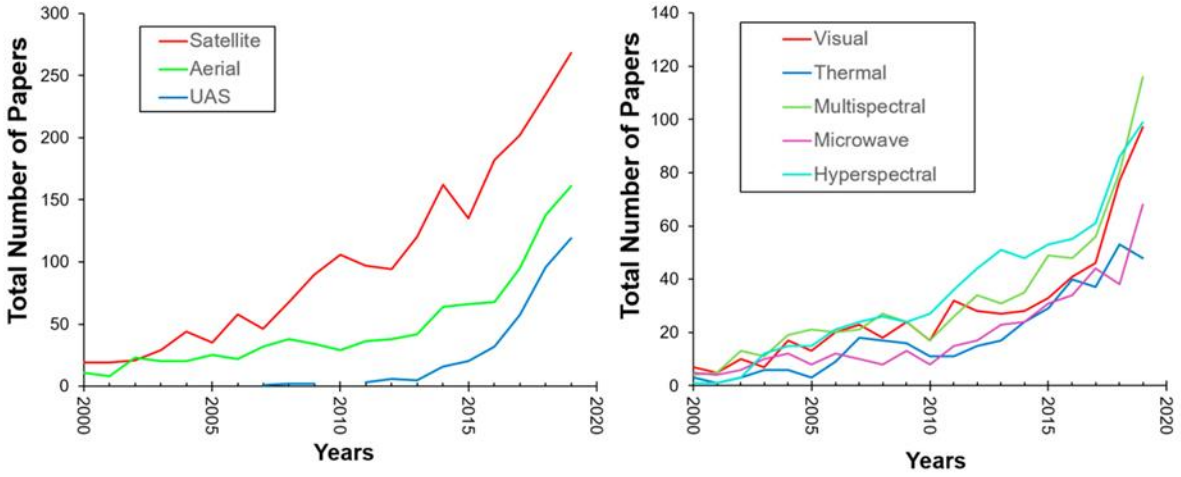

Figure 2.2. Research trends about the application of remote sensing in agriculture between 2000 and 2019 (Khanal et al., 2020)

Even though RS has been extensively used in different sectors, its application on agricultural farms is minimal (Tenkorang & Lowenberg-DeBoer, 2008). Some of the remote sensing applications in agriculture include providing data (weather, area, yield), monitoring crop growth, soil moisture content, and crop disease infestations (Liaghat & Balasundram, 2010; Moussaid et al., 2021; Shanmugapriya et al., 2019).

Frequent monitoring of the crop condition is essential during its growth period. Space mounted remote sensing, or an Unmanned Aerial Vehicle (UAV) method, is highly suitable for continually monitoring crop conditions (Ray, 2016).

The radiometric approach is mainly used for mapping crop types and the area of the cropland. Several reports showed that Remote Sensing has the potential to identify the crop variety, double cropping, sowing and harvest date, tillage, row orientation, and width (Aguiar et al., 2011; Arvor et al., 2011; Bégué et al., 2019; Léna Maatoug, Damien Arvor, Margareth Simões, 2012; Ozdogan, 2010; Sullivan et al., 2008).

Digital image analysis based on supervised or unsupervised classification algorithms is commonly used to prepare crop classification maps and characterize cropping practices (Nellis et al., 2009). Nellis (1986) applied the maximum likelihood classification approach to classify the Landsat digital images and prepare a map of the irrigated crop area. Price et al. (1997) advanced this approach by using a multi-temporal Landsat thematic mapper (TM) to map the distribution of irrigating crops. Thenkabail et al. (2004) conducted a crop classification study using data mining techniques using hyperspectral sensors within the wavelength range of 400 nm to 2500 nm. The introduction of the hyperspectral band in RS enables the preparation of a

detailed crop classification map. This technique includes analyzing the main components, using models (lambda-lambda), categorizing based on specific criteria, and developing a different vegetation index. According to Nellis et al., (2009) this hyperspectral approach increases crop classification map accuracy by up to 43%.

Plants have a slow response in the red band wavelength region as they absorb incident radiation by chlorophyll pigments. In contrast, plants have a high response rate for Near-Infrared bands (NIR) due to the high reflection of radiation. The vegetation conditions can be evaluated by developing different indices based on various multispectral bands and the related plant response (Xue & Su, 2017). The application of different vegetation indices such as Normalised Difference Vegetation Index (NDVI), Enhanced Vegetation Index (EVI), and greenness index has been accepted as a reliable approach to monitoring the growth of the plant and its condition (Shanmugapriya et al., 2019). The water content can be determined using a Normalized Difference Water Index (NDWI) (Gao, 1996). The green and red chlorophyll index (CHLG and CHLR) are also used to estimate the leaf chlorophyll content (A. Gitelson et al., 2003). The Enhanced Vegetation Index (EVI) is a modification of NDVI that aims to optimize the spectral signatures of the vegetation with a high leaf area index (A. Huete et al., 2002). The Green Normalized Difference Vegetation Index (GNDVI) is like NDVI with a difference in the use of green wavelength instead of red wavelength (A. A. Gitelson et al., 1996). The Modified Chlorophyll Absorption Index is the narrow band vegetation index, which estimates the relative chlorophyll concentration (Daughtry et al., 2000). The Simple Ratio (SR) and the Soil Adjusted Vegetation Index (SAVI) are the broadband vegetation index used to characterize the green biomass of the target area (Blackburn, 1998; A. R. Huete, 1988). The structure Intensive Pigment Index (SIPI) is used to estimate canopy and leaf carotenoids (Penuelas et al., 1995). The vegetation indices used in this study are summarized in Table 2.2 below.

Table 2.2. The different types of vegetation indices used for the study

Index	Symbol	Formula	Applications	Source/Reference	Remark
Chloropropyl index Green	CHLG	(R800/R550)-1	Chloropropyl content	Gitelson et al., (2003)	
Chloropropyl index Red	CHLR	(R800/R670)-1	Chloropropyl content	Gitelson et al., (2005)	
Enhanced Vegetation Index	EVI	2.5*(R800 - R670) / ((R800 + 6*R670)) - (7.5*R490)+1)	Green biomass and phenology	Huete et al., (2002)	Range from -1 to 1. The typical range for green vegetation is 0.2 to 0.8
Green Normalized Difference Vegetation Index	GNDVI	$\frac{R800 - R550}{R800 + R550}$	Vegetation condition	Gitelson et al., (1996)	Range from -1 to 1.
Modified Chlorophyll Absorption Ratio Index	MCARI	((R700 – R670) – 0.2 * (R700 – R550)) * (R700 / R670)	relative abundance of chlorophyll	Daughtry et al., (2000)	
Normalized Difference Vegetation Index	NDVI	(R800 – R680) / (R800 + R680)	Level of greenness, Biomass, health	Rouse et al. (1974), as cited in Xue and Su (2017)	Range from -1 to 1. The typical range for green vegetation is 0.2 to 0.8
Normalized Difference Moisture Index	NDMI	$\frac{R820 - R1600}{R820 + R1600}$	Water content, canopy stress, plant productivity	Gao, (1996)	Range from -1 to 1. The typical range for healthy canopy cover is 0 to 0.8.
Simple Ratio	SR	$\frac{R800}{R670}$	Green biomass	Blackburn, (1998)	
Soil Adjusted Vegetation Index	SAVI	1.5*(R800 – R670) / (R800 + R680+0.5)	Green biomass	Huete, (1988)	Range from -1 to 1.
Structure Insensitive Pigment Index	SIPI	$\frac{R800 - R445}{R800 + R680}$	Canopy and leaf carotenoids	Penuelas et al., (1995)	Range from 0 to 2. The common range for green vegetation is 0,8 to 1,8/

2.3. Leaf Spectral Response

Detecting the abiotic or biotic plant stresses at the early growth stage is vital to take the necessary intervention on time and thus prevent yield loss (Wasonga, 2021). The conventional approach to assessing plant physiology conditions is laborious and time-consuming. It does not allow repetitive measurement on the same plant (Walter et al., 2015). Recently, non-destructive optical sensors have proved effective for continuously monitoring plant growth and detecting potential plant stress.

Plant imaging detects physiological changes through plant response to absorbed, reflected, and transmitted light (Li et al., 2014). The spectral response of plant leaves is determined by the leaves' physiological characteristics, which can be detected in the ultraviolet, visible, and infrared wavelength regions. The primary leaf pigments: chlorophyll, carotenoids, and xanthophylls, have their unique spectral responses. The change in the spectral response of those leaf pigments can be used to detect the condition of the plant (Wasonga, 2021).

One of the most common approaches to determining the spectral properties of plants is the use of spectroradiometers. The field and laboratory spectroradiometers can provide measurements with a wavelength range of 300 to 1100 nm (MacArthur et al., 2012). The CI-710s SpectraVue Leaf Spectrometer is among the popular spectroradiometers (Wasonga, 2021). It is designed to simultaneously measure the absorption, transmission, and reflection of light by a plant over a wide wavelength range. The latest SpectraVue Leaf Spectrometer has been upgraded with new features, including a wide wavelength range (360-1100 nm), leaf probe attachment, a built-in window-based operation system, and a touch screen. This makes the sensors portable and time-saving. Two broadband light sources are attached to the leaf spectrometer. The one found in the leaf clamp is for measuring the light transmission, while the other one positioned inside the case is for measuring the amount of light to be reflected. The device receives light from the leaf probe attachment and projects the wavelength light onto a CCD array. Each pixel of the CCD array thus corresponds to a specific wavelength of light (CID Bio-Science, n.d.).

2.4. Related Previous Studies

Several studies have been conducted to assess the potential application of open data satellite images (Sentinel 2 or Landsat 9) in estimating the biophysical properties of plants. However, only a few highlighted the comparison of different sensors against the field measurement. Some of these reports are discussed in the following paragraphs.

Davis (2018) compared the performance of Landsat 8 (OLI) and Sentinel 2A (MSI) sensors in estimating the soil salinity using spectral, statistical, and image analysis approaches. To compare the performance of the sensors, the Electrical Conductivity (EC) of the sampled soils has been correlated with the multispectral bands. Coefficient of Determination (R^2) and Root Mean square Error (RMSE) have been used for statistical analysis. The study revealed that the finer resolution Sentinel 2 bands provide more accurate estimates of soil salinity than the Landsat OLI bands.

García-Llamas et al. (2019) evaluate the potential application of Landsat 8, Sentinel 2, and Deimos 1 remote sensing platforms in detecting the burn severity of the Spain Mediterranean ecosystem. A total of 13 vegetation indices have been used and validated against the severity matrix according to the CBI index. The correlation pattern among the burn severity and vegetation indices was consistent for all sensors, even though the Sentinel 2 performed slightly better than the other two sensors.

Darvishzadeh et al. (2019) mapped the chlorophyll content of the Norway Spruce using the Sentinel 2 and RapidEye data and INFORM and RTM models. R^2, RMSE, and NRMSE have been used for statistical analysis. A strong correlation has been observed between the simulated and measured reflectance of Sentinel 2 and RapidEye. The statistical analysis also showed that Sentinel 2 has a better performance than RapidEye.

Korhonen et al. (2017) assessed the performance of Sentinel 2 and Landsat 8 in estimating the Canopy Cover and Leaf Area Index (LAI) of the boreal forests. Both airborne lidar data and field plots were used to determine the CC and LAI. RMSE has been used as an efficiency criterion. According to the statistical analysis, Sentinel 2 had a better performance than Landsat 8.

3. MATERIALS AND METHODS

3.1. Description of the Study Area

The study was conducted on a farm plot found 1.5 km from the village of Ovcha Mogila (Figure 3.1). It is located in the central part of the Danube hilly lowland, about 20 km south of the city of Svishtov, 3 km from northeast of Levski, and 48 km from northwest of Veliko Tarnovo (Wikipedia, 2022). The area has a temperate continental climate with an average temperature of 1ºC during winter and 22 ºC during summer. The site has mean annual precipitation of 615 mm. Ovcha Mogila is found mainly in flat terrain in the broad valley of river Barata with an average altitude of 80 m.

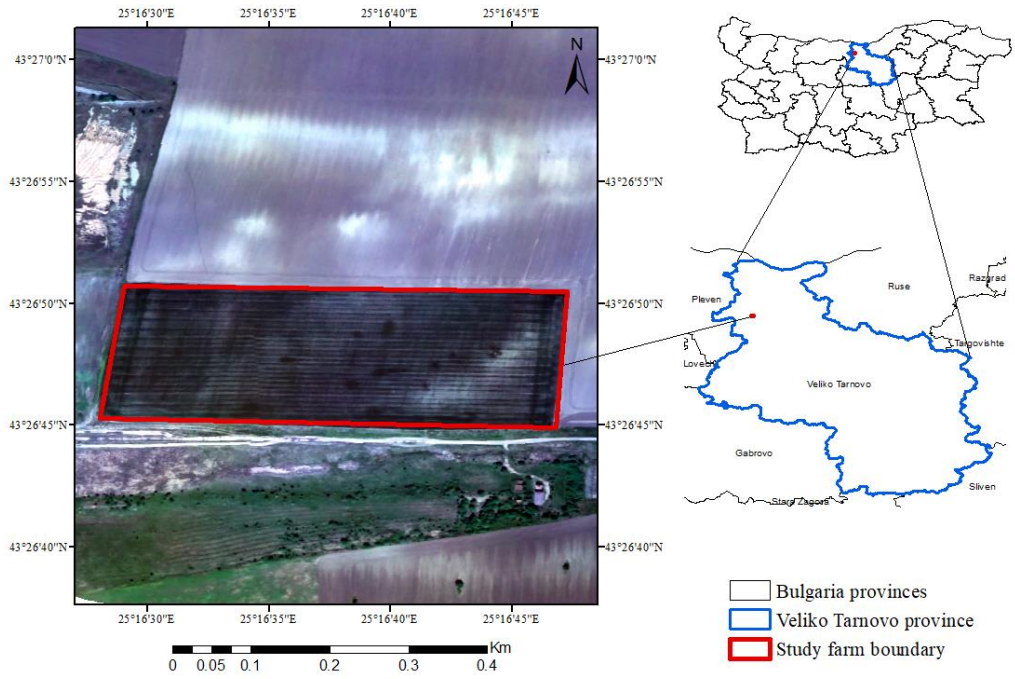

Figure 3.1. Location map of the study farm plot

3.2. Methodology

We employed satellite image analysis and *in-situ* field measurement techniques to answer the main research questions of this study. A Landsat 9 (USGS, 2013) and Sentinel-2 satellite images have been gathered from the open data source for five consecutive months. The satellite images with less than 10% cloud cover have been selected for this study. Ten most common vegetation indices have been selected. Based on the reflectance wavelength range, the vegetation indices have been determined. Besides, soil data has been collected in eight different locations within the farm plot. The different physicochemical properties of the soil (pH, texture,

N, P_2O_5, and K_2O) have been analyzed in the laboratory. Moreover, a SpectraVue Leaf Spectrometer was used to measure the spectral response of the crop in April at five different locations within the farm. A Buteo drone (http://prodronesys.com/hexacopter) has also been used to capture the spectral response of the plant leaves. A statistical analysis (coefficient of determination (R^2) and root mean square error (RMSE)) and correlation matrix using heatmap python library were used to compare the performance of Landsat9, Sentinel2, the Buteo drone, and the Leaf spectrometer in determining the biophysical properties of the wheat crop. The general methodology of the study is outlined in Figure 3.2.

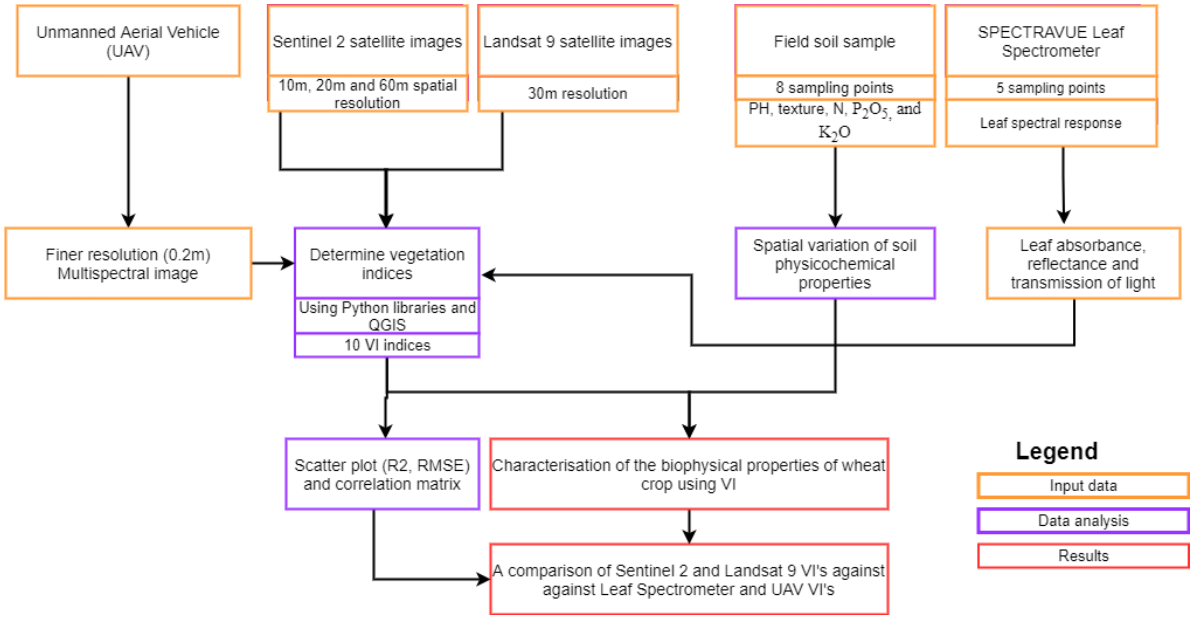

Figure 3.2. General approach of the study

3.3. Field Setup and Sampling

The wheat crop was sown in the study farm plot in October 2021. To characterize the soil physico-chemical properties, soil samples with a weight of 1 kg per sampling point have been collected from eight sampling locations. The sampled soil has been analyzed in the laboratory to determine the pH, soil textural fractions, N, P_2O_5, and K_2O. The soil pH was measured with a digital pH meter. The available nutrients have been determined using the methods discussed in Verma et al. (2018). A soil texture has been determined based on textural soil fractions using the United States Department of Agriculture soil textural classifications approach (USDA, 1987). The value of soil parameters has been interpolated spatially to develop a spatial soil properties map. The different spatial interpolation techniques have been compared with the efficiency criteria of RMSE. Even though kriging has the lowest RMSE, as the number of sampling points were minimum it didn't interpolate successfully. Due to this the Inverse Distance Weighting method has been selected.

3.4. In-situ Field Measurement

The spectral response of the plant leaves has been measured using the CI-710s SpectraVue Leaf Spectrometer. This optical sensor is designed to measure simultaneously the absorption, transmission, and reflection of light by a plant using its attached leaf probe over a wide wavelength range (360-1300 nm). The leaf spectral response has been measured at 5 points inside the farm plot. The spectral values have been used to determine the selected vegetation indices according to their empirical formula (Table 2).

3.5. Remote Sensing Data

The Landsat 9 satellite images have been collected from the USGS Erath Explorer open data source (https://earthexplorer.usgs.gov) from January to April. The satellite images have been downloaded by setting cloud cover criteria of less than 10%. There were no images from Landsat 9 for January based on these criteria. The Landsat 9 has nine bands with a spatial resolution of 30 m except for the panchromatic band (15 m) and thermal infrared band (100 m).

A scale factor of Landsat 9 (collection 2, level 2 data) was performed before it was used to determine the vegetation indices. The scale factor has been done according to Sayler & Zanter (2022) with a multiplicative scale factor of 0.0000275 and additive offset of 0.2.

The Sentinel satellite images have been downloaded from the Copernicus open hub website (https://scihub.copernicus.eu/dhus/#/home) for the period from November to April. The Sentinel-2 (S2MSI) images have 13 bands with different spatial resolutions. The sensor has a spatial resolution of 10 m, 20 m, and 60 m. Similarly, a cloud cover percentage of less than 10% was applied to gather quality satellite images for further analysis (Table 3.1).

Besides, Unmanned Aerial Vehicle (UAVs) has also been used to collect multispectral images. Because of the relatively high cost of the data collection, the Buteo drone (http://prodronesys.com/hexacopter) scanning was done only once in April. The multispectral bands collected from UAV have been mosaicking and geo-rectified using the Pix4D software. The UAV images within the visible and near-infrared range have been used to determine the selected vegetation indices.

Table 3.1. the Landsat 9 and Sentinel 2 satellite images used for the study

Landsat 9			Sentinel 2		
Sensing date	Sensor	Spatial resolution	Sensing date	Sensor	Spatial resolution
24/12/2021	OLI-2	30m	19/12/2021	MSIS2B	10m/20m/60m
			20/01/2022	MSIS2A	10m/20m/60m
10/02/2022	OLI-2	30m			10m/20m/60m
26/02/2022	OLI-2	30m	19/02/2022	MSIS2A	10m/20m/60m
30/03/2022	OLI-2	30m	21/03/2022	MSIS2A	10m/20m/60m
			05/04/2022	MSIS2B	10m/20m/60m
15/04/2022	OLI-2	30m	13/04/2022	MSIS2A	10m/20m/60m

3.6. Data Analysis

Prescreening and clipping of the satellite images according to the study area boundary have been carried out using QGIS software. For the purpose of minimizing errors during further analysis, the courser resolutions Sentinel-2 bands (20 m and 60 m) have been resampled to 10 m using QGIS.

The ten most common broadband and narrowband vegetation indices have been selected, as summarized in Table 2. Based on the wavelength range of each satellite band, the vegetation indices have been determined according to their empirical equations. The Jupiter Notebook and its built-in Python program have been used to determine the vegetation indices. Several python libraries have been used, including NumPy, Pandas, Matplotlib, and Rasterio. The map layout has been done using ArcMap version 10.5. The measured leaf spectral responses in terms of reflectance, transmission, and absorption have been used to determine the selected vegetation indices. The temporal trend of vegetation indices has been analyzed from December to April.

The soil physicochemical properties and the measured leaf spectral response have been used as a standard to compare the accuracy of satellite images and drones in determining wheat crop biophysical properties. Each vegetation index was determined using the bands of Landsat 9 or Sentinel-2 and has been compared against the vegetation indices of the drone. Besides the vegetation indices of Sentinel 2, Landsat 9 and Drone have been extracted to the sampling 5 locations using the spatial analyst tool of ArcMap and compared with the vegetation indices of Leaf Spectrometer. All the vegetation indices images have been resampled to 10 m to perform further statistical analysis. A scatter plot has been used to compare Sentinel 2, Landsat 9, and Drone vegetation indices. The coefficient of determination (R^2) and Root Mean Square Error (RMSE) have been used as comparison criteria. Besides, a correlation matrix has been prepared using a corr and the seaborn heatmap python libraries. A correlation matrix has been prepared

among the vegetation indices of different sensors as well as with the different physicochemical properties of the soil. A Pearson correlation coefficient (r) has been used to assess the correlation matrix.

$$R^2 = \frac{\sum\left(\left(Rmeasured - \overline{Rmeasured}\right)\left(Rmodeled - \overline{Rmodeld}\right)\right)^2}{\sum\left(Rmeasured - \overline{Rmeasured}\right)^2 \sum \left(Rmodeled - \overline{\overline{Rmodeld}}\right)^2} \quad (1)$$

$$RMSE = \sqrt{\frac{\sum(Rmeasured - Rmodled))^2}{n}} \quad (2)$$

$$\mathrm{r} = \frac{\sum\left(\left(Rmeasured - \overline{Rmeasured}\right)\left(Rmodeled - \overline{Rmodeld}\right)\right)}{\sqrt{\sum\left(Rmeasured - \overline{Rmeasured}\right)^2 \sum \left(Rmodeled - \overline{\overline{Rmodeld}}\right)^2}} \quad (3)$$

Where $R_{measured}$ is the measured reflectance value measured by either of Sentinel 2, Landsat 9, Drone and Leaf Spectrometer. $R_{modeled}$ is the predicted reflectance value of the sensors to be compared against a specific sensor.

4. RESULTS AND DISCUSSION

4.1. Physio-chemical Properties of Soil Samples

The spatially interpolated physio-chemical properties of the soil are portrayed in Figures 4.1 and 4.2. Most of the study area has a pH value between 8.4 to 8.52. The maximum available nutrients are observed to be concentrated in the Northeast part of the study area. The north and northeast part of the study area is dominated by sand and silt fraction, while the northwest and central part of the study farm has a significant clay fraction. According to the USDA soil textural classification, the study farm is dominated by Clay and Clay Loam soil texture.

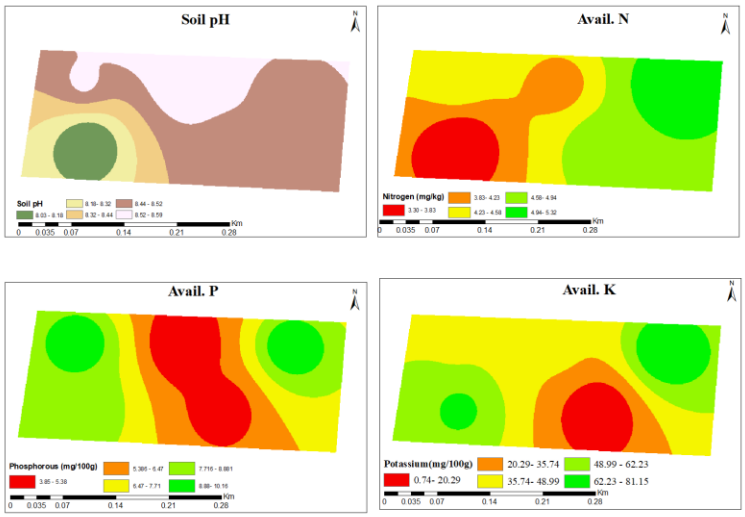

Figure 4.1. Spatial interpolation from the properties of collected soil samples

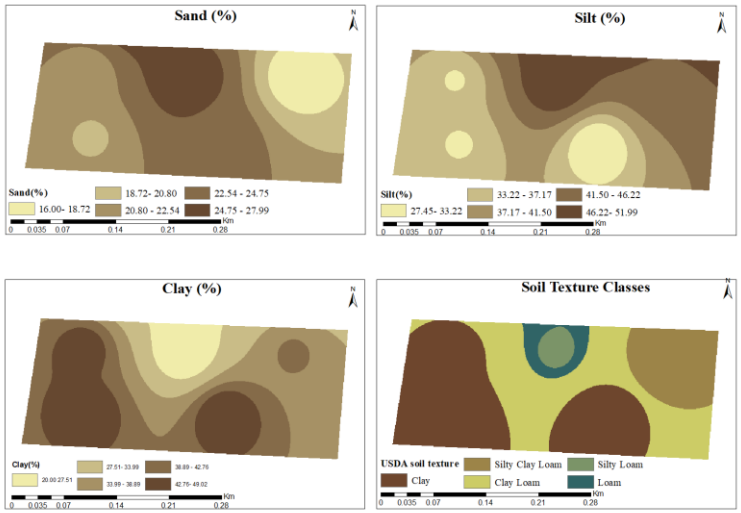

Figure 4.2. Interpolated spatial distribution of soil texture in the study area

4.2. Vegetation Indices using Leaf Spectrometer

Figure 4.3 shows the vegetation indices (NDVI, EVI, GNDVI, CHLG, CHLR, SAVI, SIPI, SR) determined based on the reflectance values of the study wheat leaves. As the vegetation indices from the measured leaf spectral response at five sampling points do not include the data from soil reflectance, the vegetation indices did not successfully represent the lower range of values determined by the remote sensing tools. For all the vegetation indices, the highest values were observed in the northern part of the study area, while the minimum values were detected in the northeast and southwest part of the farm. Because of its coarse interpolation, the spectrometer vegetation indices have not been used to compare against the vegetation indices of other sensors. In similar research, Yang et al. (2011) pointed out that having a representative spectral value of different Earth features improves the accuracy of spatial interpolation of the vegetation indices. As the Leaf Spectrometer is intended to measure the spectral response of the plant leaves, its application for a representation of spectral values of the whole farm field is limited.

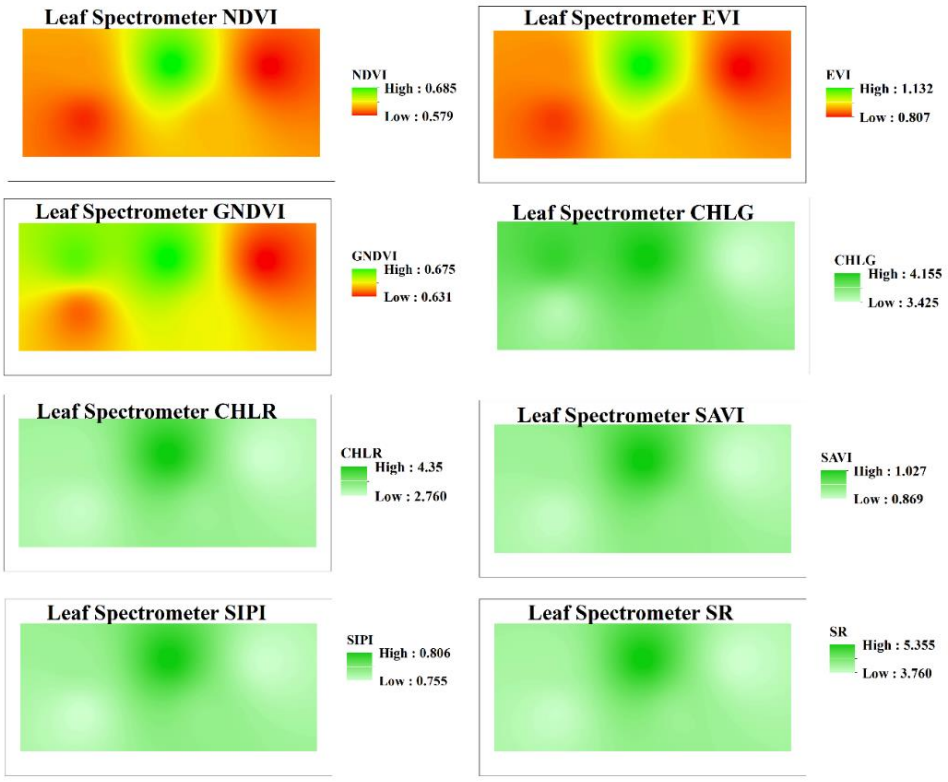

Figure 4.3. The different vegetation indices determined based on the output of leaf spectrometer

4.3. Vegetation Indices using Buteo drone

The vegetation indices determined based on the spectral values of the fine resolution UAV are presented in Figure 4.4 – most of the vegetation indices are within the standard range. The maximum values of the vegetation indices have been observed in the north and southeast parts of the study area. Minimum vegetation indices were observed in an area where the available nitrogen was lower. Several studies (Gozdowski et al., 2020; Mashonganyika et al., 2021; Thapa et al., 2019) have shown that the NDVI value of a matured wheat crop depends on several factors, including variety and climate. For most varieties of matured wheat, the NDVI values range from 0.4 to 0.8. This strongly aligns with the NDVI values of the study area around its maturity in April.

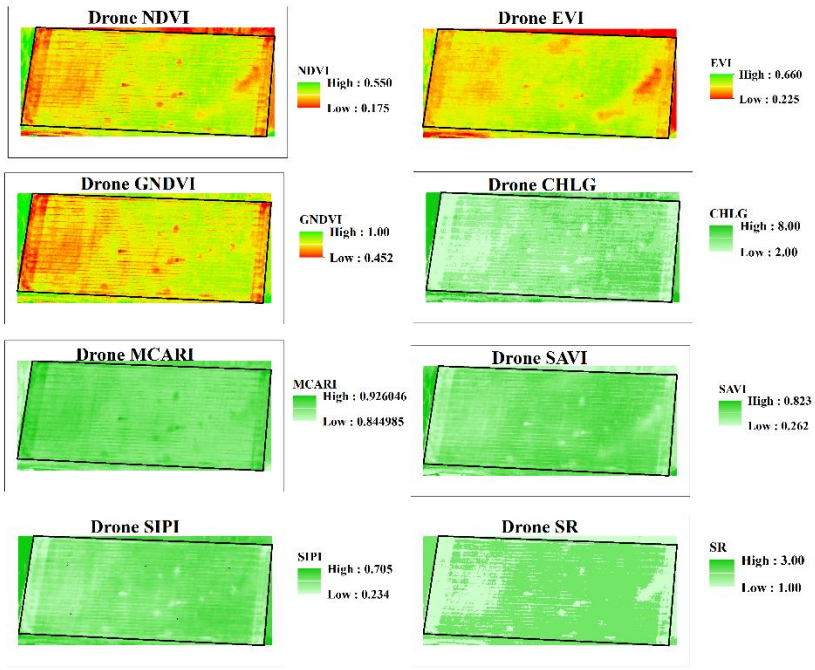

Figure 4.4. The different vegetation indices determined based on the output of the drone.

4.4. Vegetation Indices using Sentinel 2 and Landsat 9

Figures 4.5 and 4.6 present the green chlorophyll index for the months between December and April determined using the spectral values of Sentinel 2 and Landsat 9 sensors. The CHLG determined using the Landsat 9 images showed a linear increase with the growing days of the plant. On the other hand, the CHLG determined based on the Sentinel 2 images showed an increasing trend between December and January and then decreased in February and March until it rose again in April.

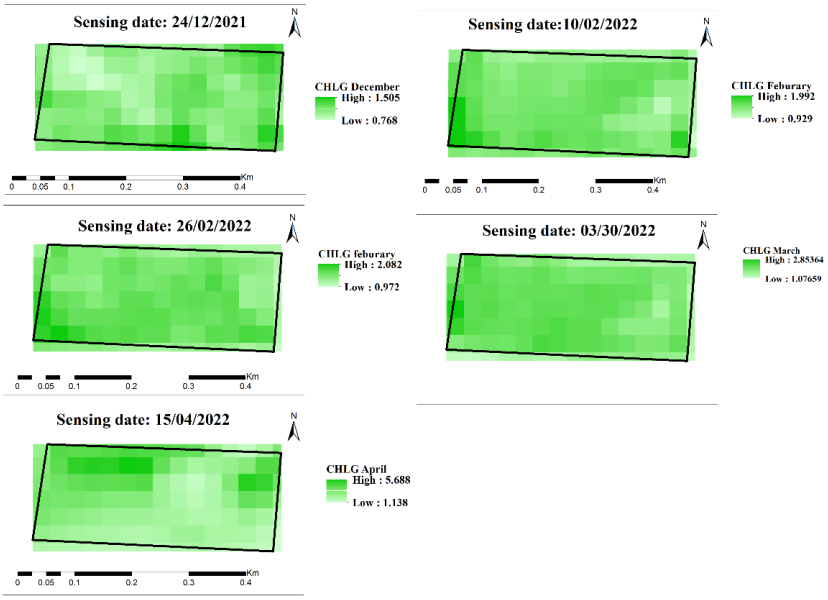

Figure 4.5. Chlorophyll Index Green based on Landsat 9 images

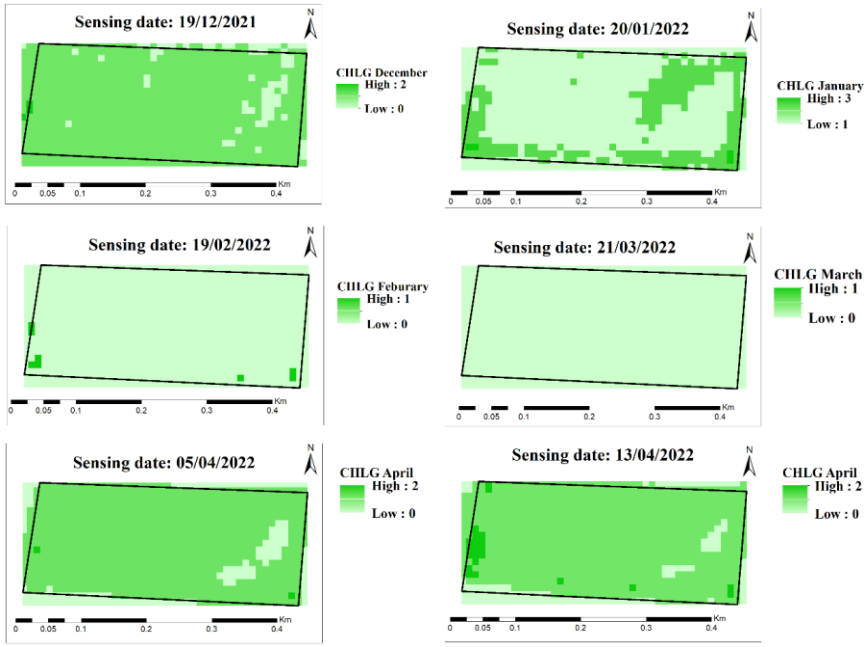

Figure 4.6. Chlorophyll Index Green based on Sentinel 2 images

Figures 4.7 and 4.8 show the red chlorophyll index determined using the Sentinel 2 and Landsat 9 images. As in the case of CHLG, the CHLR values showed an increasing trend over the growing seasons (December to April). Sentinel 2's CHLR showed a different trend with a decreasing value between February and March.

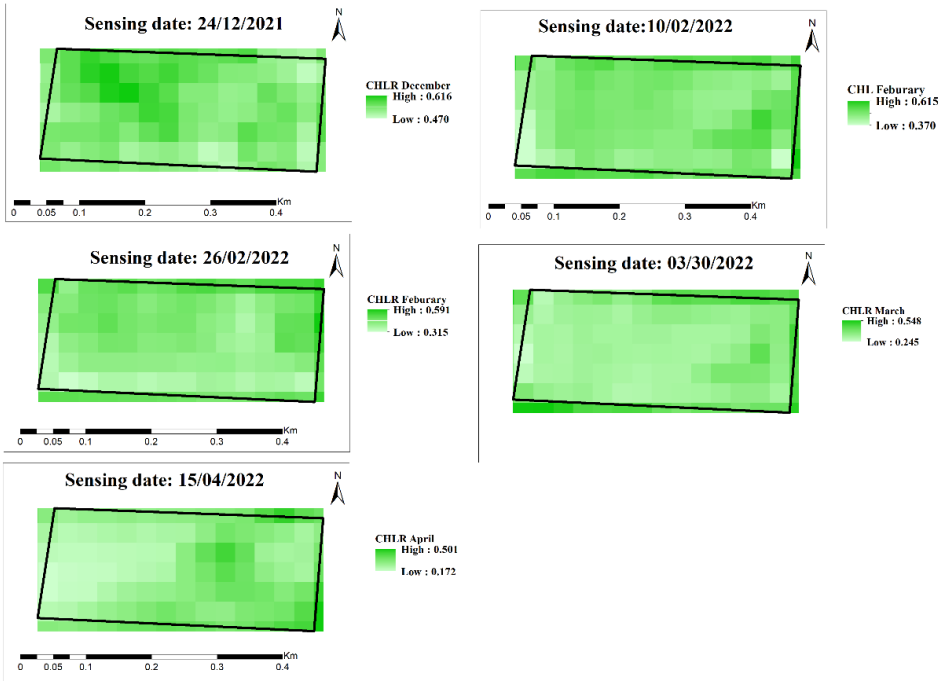

Figure 4.7. Chlorophyll Index Red based on Landsat 9 images

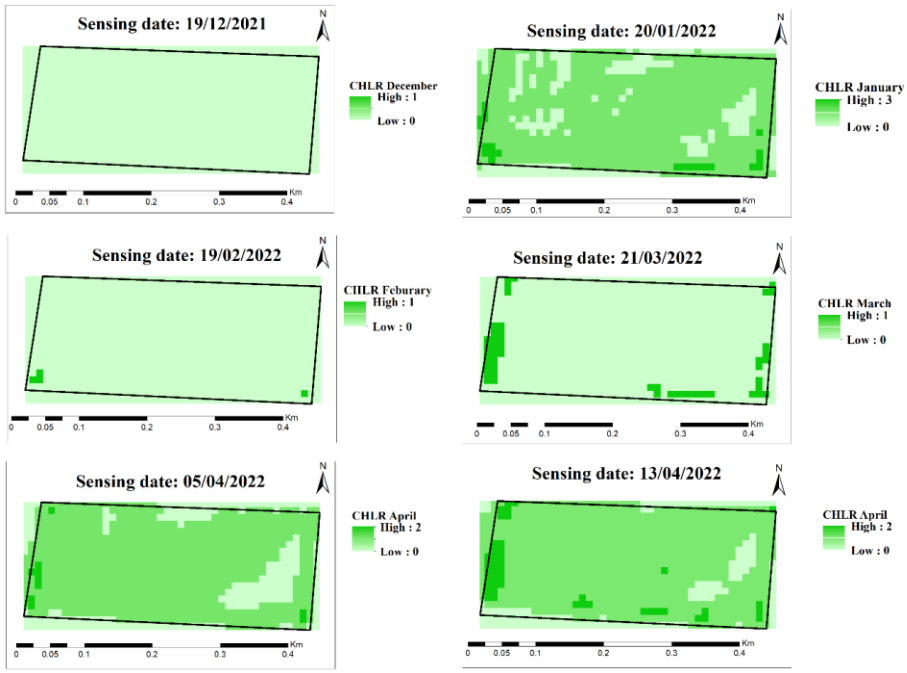

Figure 4.8. Chlorophyll Index Red based on Sentinel 2 images

The Enhanced Vegetation Index (EVI) values determined using the Sentinel 2, and Landsat 9 images are portrayed in Figures 4.9 and 4.10. The EVI values increased linearly with the crop growth. The EVI values of Landsat 9 are within the range of 0.34 to 0.50, while the Sentinel 2's EVI is outside the standard range, as high as 3.12. The maximum values were

observed in March and April for Landsat 9 and Sentinel 2 EVI maps. As discussed by Kamenova & Dimitrov (2021) and Huete et al. (2002), the EVI range of a healthy plant is within 0.2 to 0.8. The result of the study is different from other similar studies. Even though Huete et al. (2002) pointed out that the EVI value can be out of range which might be due to the high reflectance in the blue wavelength range, the reason why Sentinel 2 showed higher EVI values of Sentinel 2 remains unclear and requires further investigations.

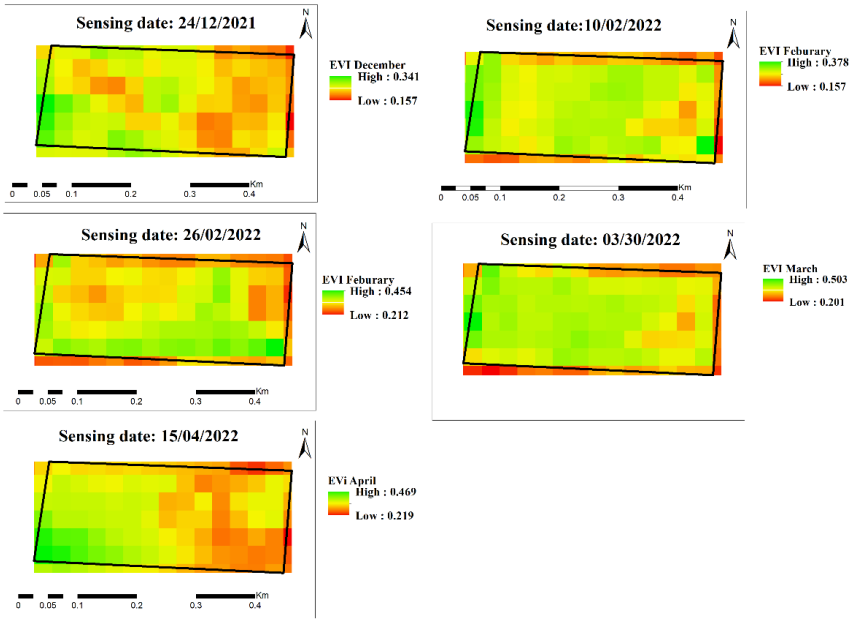

Figure 4.9. Enhanced Vegetation Index based on Landsat 9 images

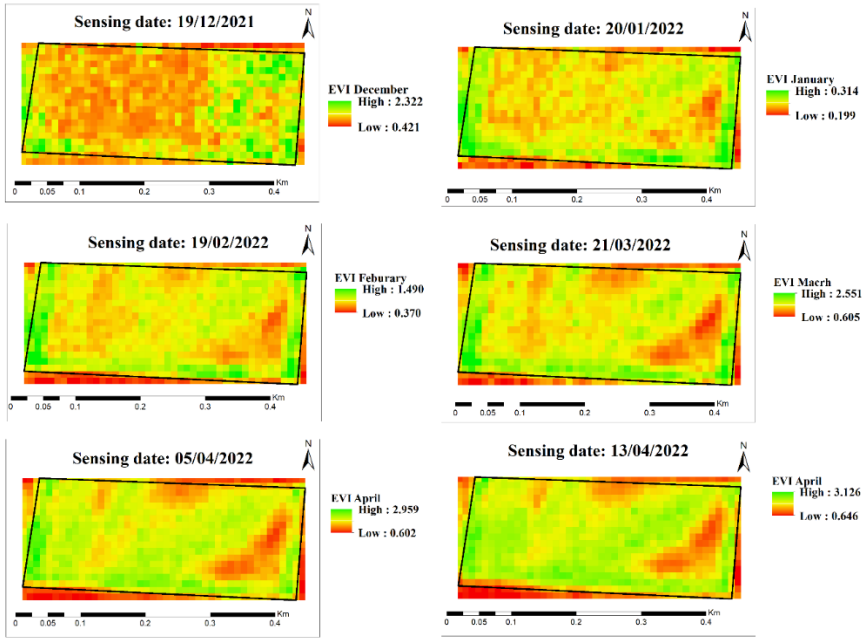

Figure 4.10. Enhanced Vegetation Index based on Sentinel 2 images

Figures 4.11 and 4.12 show the Green Normalized Vegetation index (GNDVI) map prepared using the satellite images of Sentinel 2 and Landsat 9. In both cases, the GNDVI values increased with increasing growing days between December and April, with maximum values observed in April.

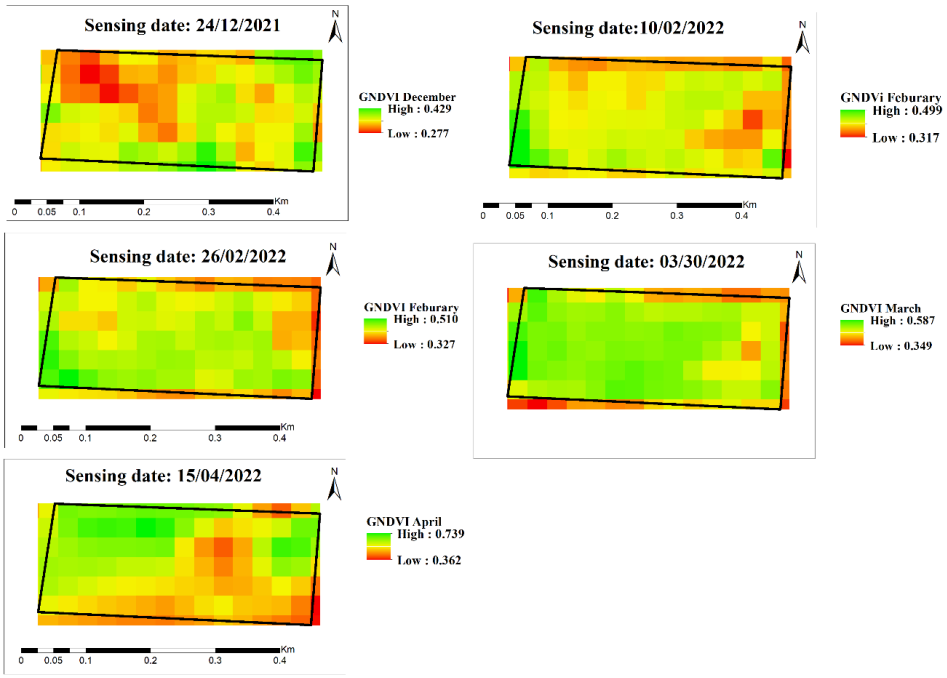

Figure 4.11. Green Normalized Vegetation Index based on Landsat 9 images

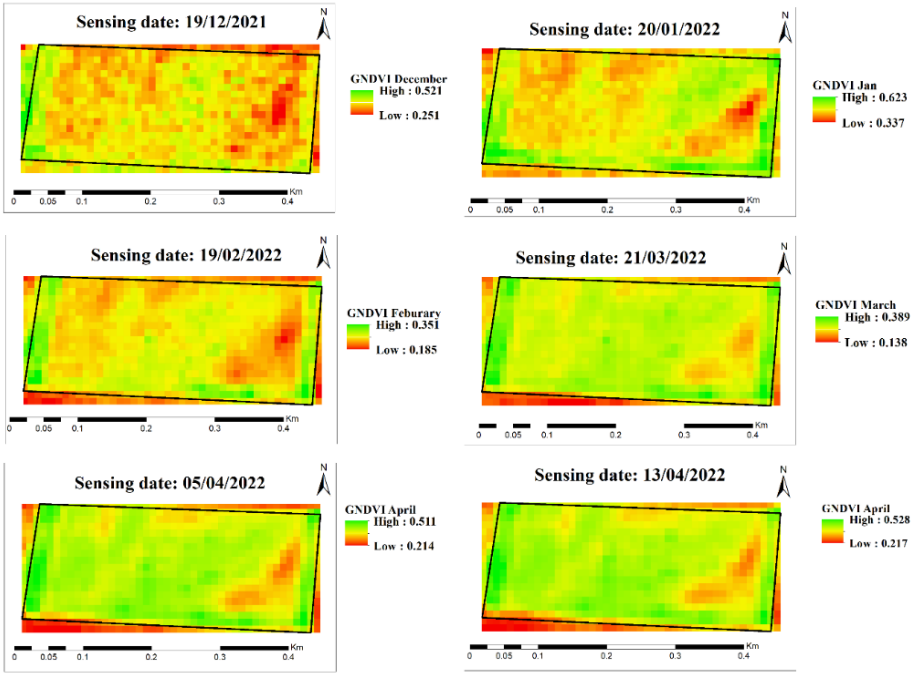

Figure 4.12. Green Normalized Vegetation Index based on Sentinel 2 images

The Modified Chlorophyll Absorption Ratio Index (MCARI) map prepared using the satellite images of Sentinel 2 and Landsat 9 is highlighted in Figures 4.13 and 4.14. The Landsat 9's MCARI values decreased over the growing season, with the highest values observed in December. Sentinel 2's MCARI values, on the other hand, were observed to be increased for the growing season, with the highest value observed in April.

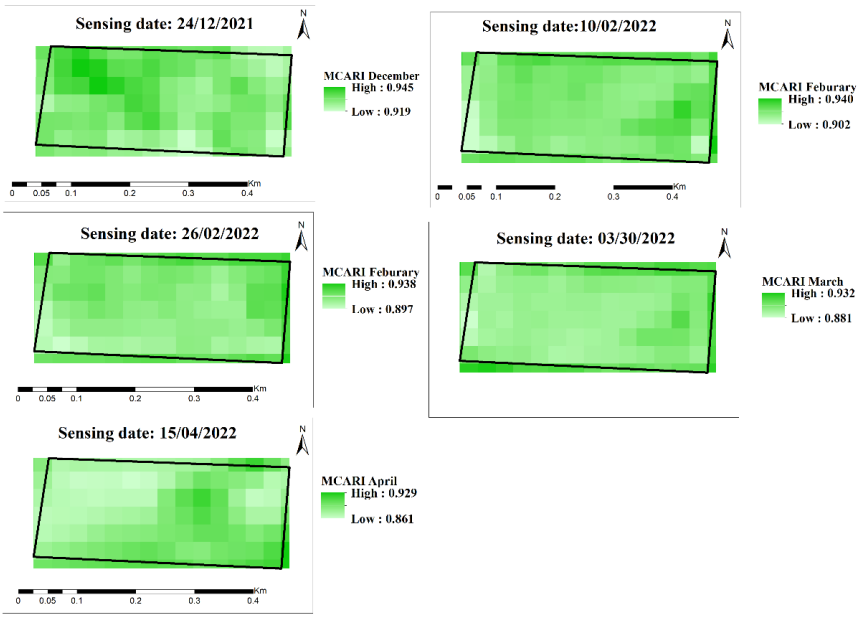

Figure 4.13. Modified Chlorophyll Absorption Ratio Index based on Landsat 9 images

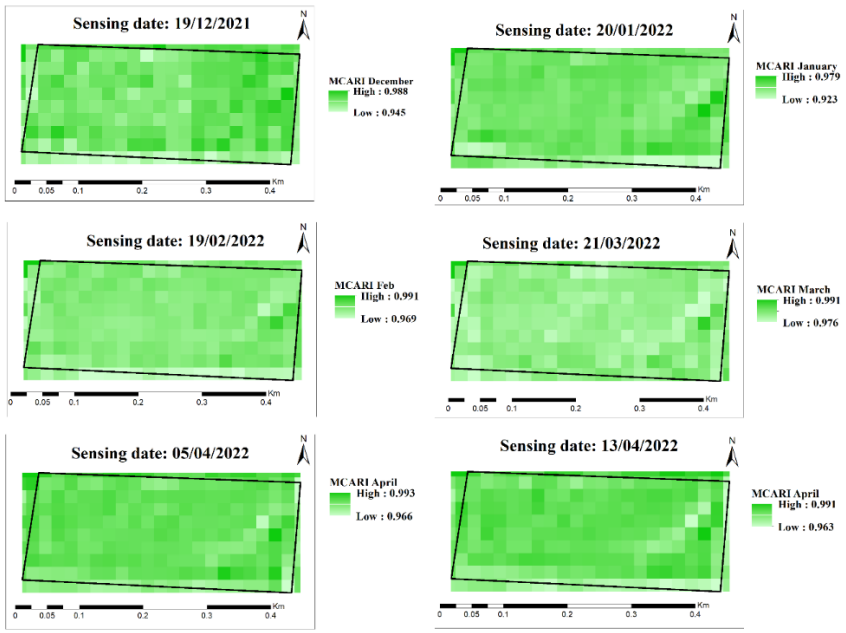

Figure 4.14. Modified Chlorophyll Absorption Ratio Index based on Sentinel 2 images

The Normalized Difference Moisture Index (NDMI) determined based on the spectral values of Sentinel 2, and Landsat 9 is presented in Figures 4.15 and 4.16. On both maps, the NDMI values increased throughout the growing season. The lower NDMI values in December and January might indicate a lower canopy cover and moisture level. The highest NDMI values in April also showed an increased canopy cover and optimum soil moisture level.

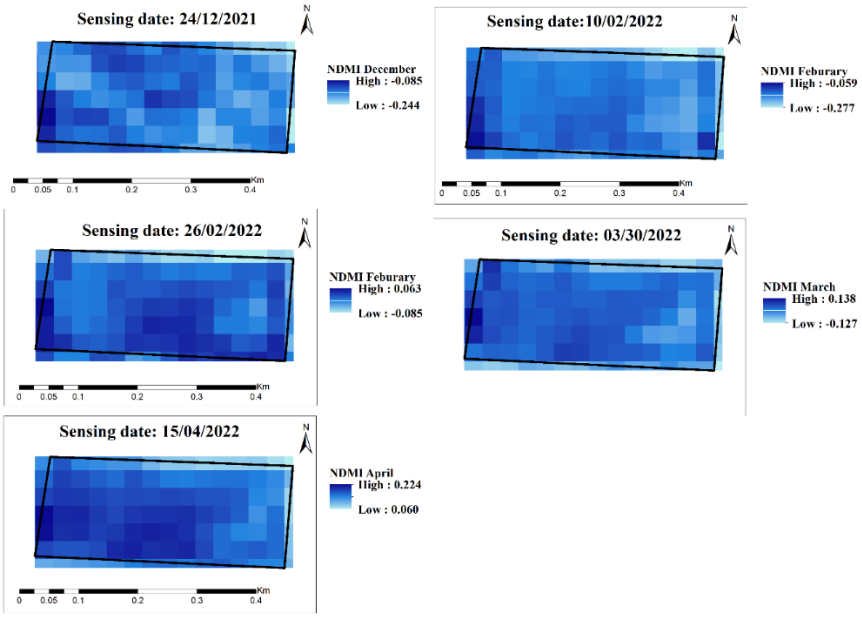

Figure 4.15. Normalized Difference Moisture Index based on Landsat 9 images

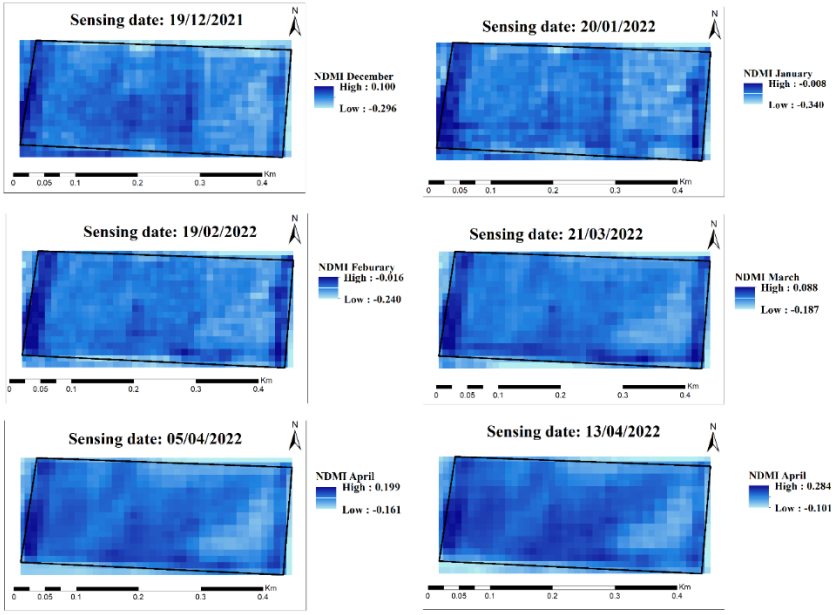

Figure 4.16. Normalized Difference Moisture Index based on Sentinel 2 images

Figures 4.17 and 4.18 highlight the Normalized Difference vegetation Index (NDVI) map prepared using the Sentinel 2 and Landsat 9 images. On both maps, NDVI values showed an increasing trend with an increase in plant growing days, with the maximum value observed in April. In relative terms, the minimum and maximum NDVI values of Landsat 9 are higher than the Sentinel 2. The maximum NDVI values were lower than the standard matured crops (0.55 to 0.70), which might indicate the crop is yet to mature.

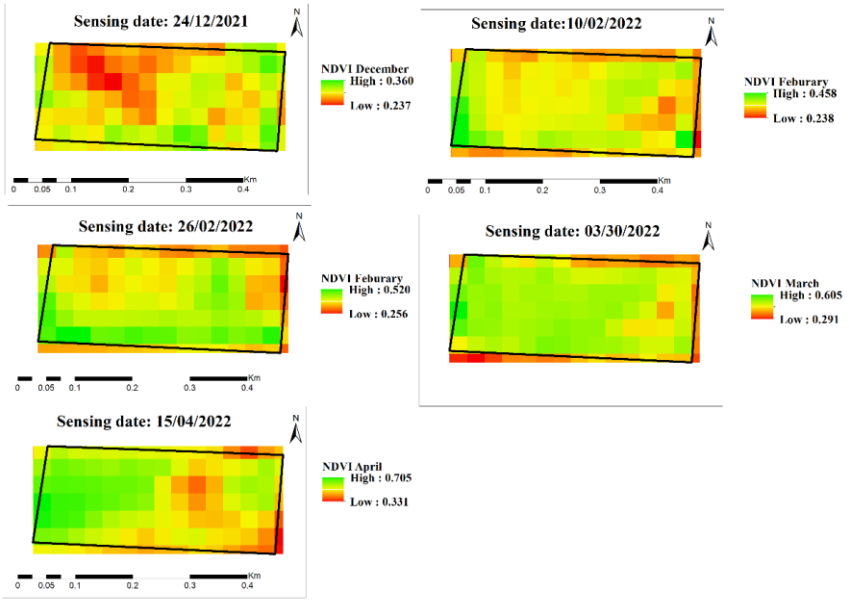

Figure 4.17. Normalized Difference Vegetation Index based on Landsat 9 images

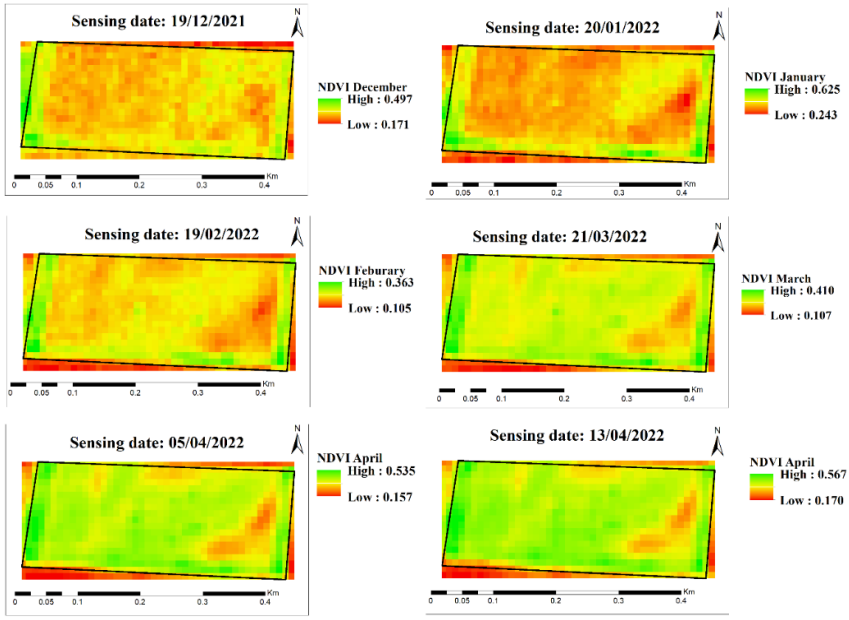

Figure 4.18. Normalized Difference Vegetation Index based on Sentinel 2 images

The Soil Adjusted Vegetation Index (SAVI) map of the study area prepared based on the spectral values of Sentinel 2 and Landsat 9 images are highlighted in Figures 4.19 and 4.20. The SAVI values range between 0.149 to 0.55 and 0.157 to 0.85 for Landsat 9 and Sentinel 2. The Landsat 9's SAVI values increased throughout the growing season, while the Sentinel 2's SAVI values decreased for February and March until it peaked in April.

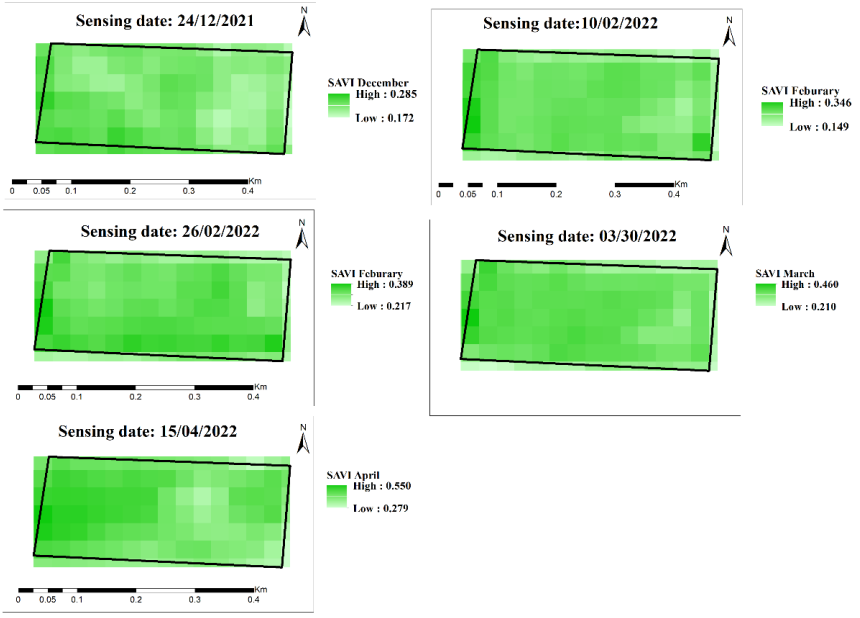

Figure 4. 19. Soil Adjusted Vegetation Index based on Landsat 9 images

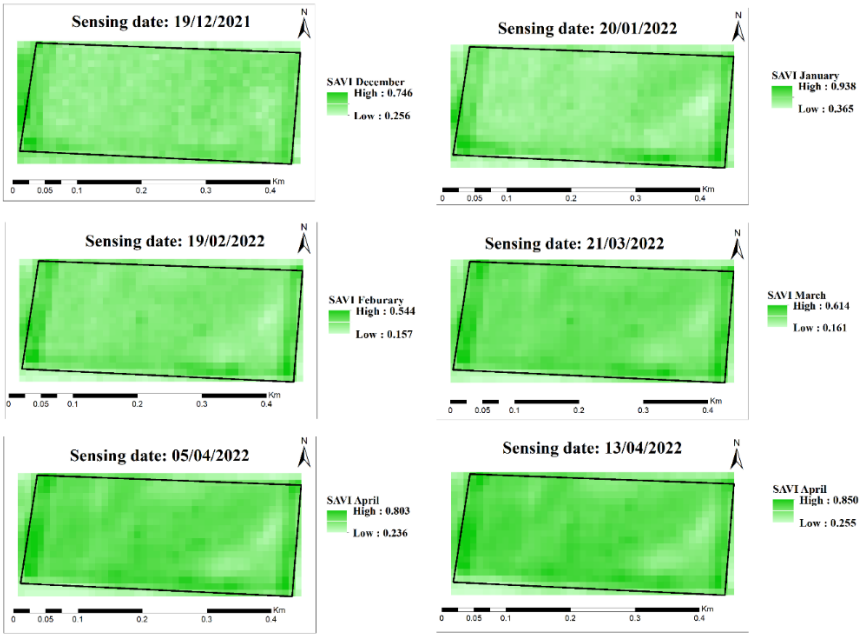

Figure 4.20. Soil Adjusted Vegetation Index based on Sentinel 2 images

The Structure Intensive Pigment Index (SIPI) map determined using Landsat 9 images highlighted a decreasing trend between December to March and then peaks in April (Figure 4.21). Figure 4.22 reveals the SIPI map determined based on the Sentinel 2 images. The value decreased linearly with an increase in growing days.

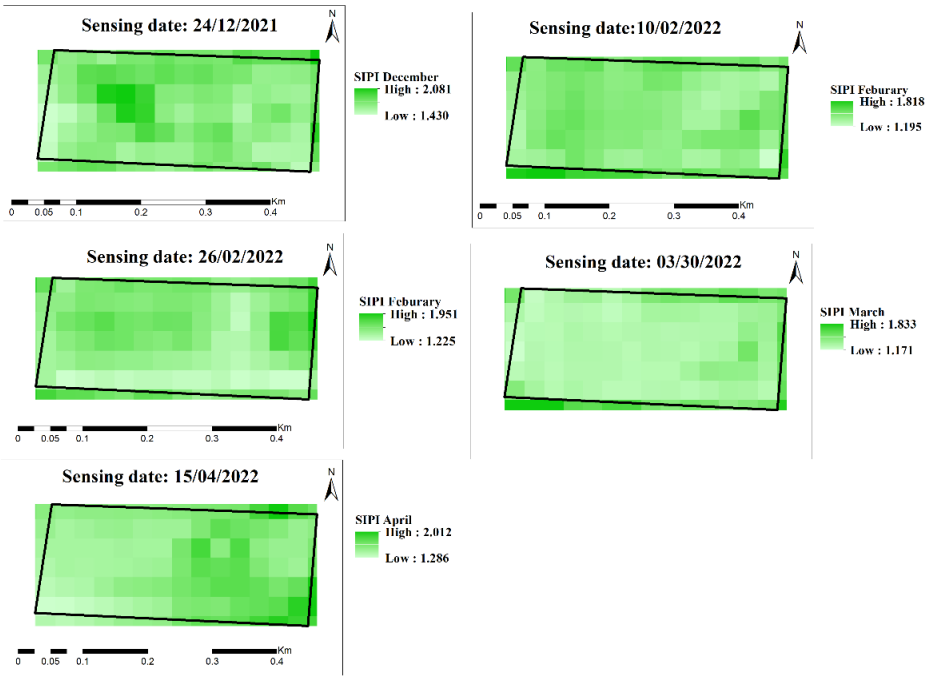

Figure 4.21. Structure Intensive Pigment Index based on Landsat 9 images

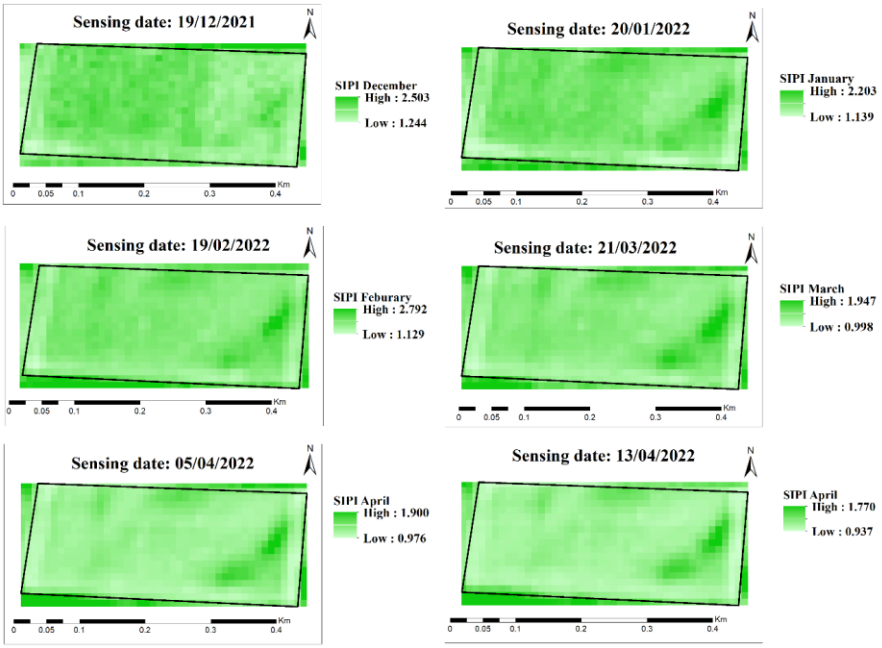

Figure 4.22. Structure Intensive Pigment Index based on Sentinel 2 images

The Simple Ratio Vegetation index (SR) map is presented in Figures 4.23 and 4.24. The SR map prepared based on Landsat 9 images showed an increasing trend over the growing season (December to April), with a maximum value observed in April. Sentinel 2's SR decreased between February and March until it rose in April.

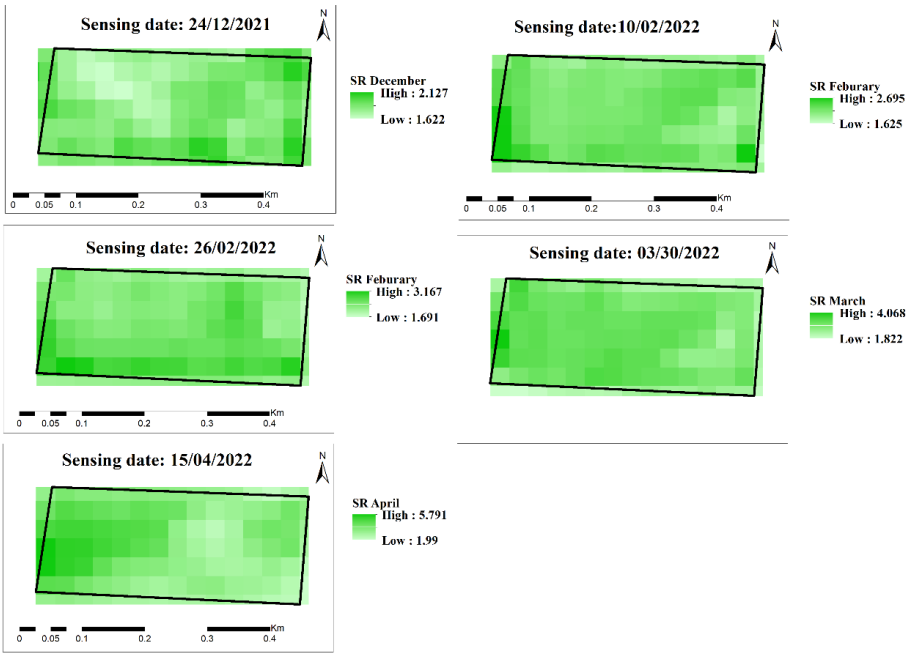

Figure 4.23. Simple Ratio Vegetation Index based on Landsat 9 images

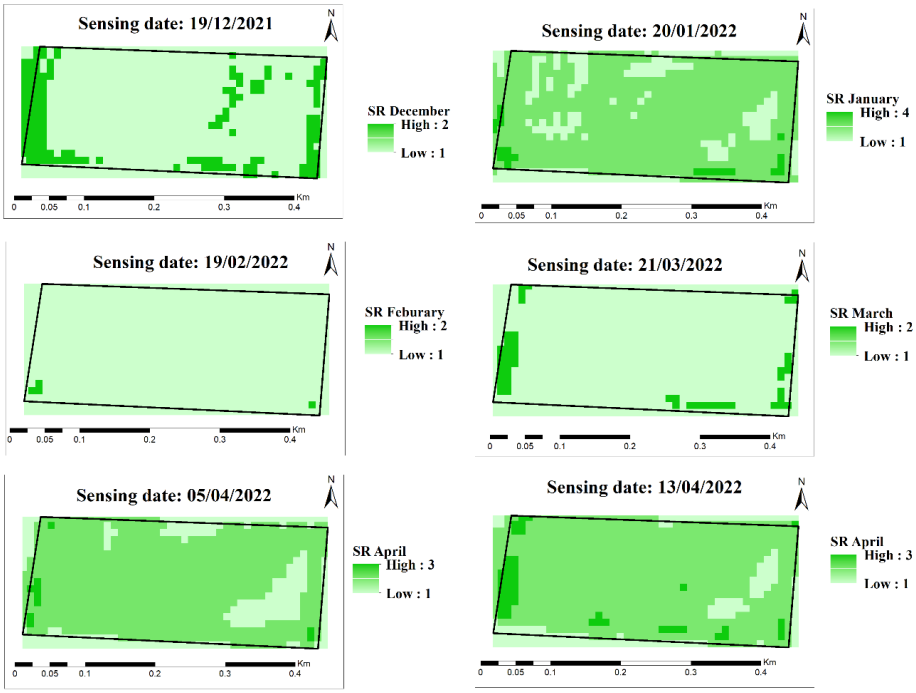

Figure 4.24. Simple Ratio Vegetation Index based on Sentinel 2 images

4.5. Performance Comparison of Sensors

The vegetation indices of Sentinel 2, Landsat 9 and Buteo drone were extracted to the soil sampling 5 points and compared against the vegetation indices based on the measured spectral response using the leaf spectrometer (Figure 4.25). The figure revealed that the Sentinel 2 and Buteo drone showed a good agreement for vegetation indices. This is expected as both Sentinel 2 and Drone have a finer spatial resolution. The Landsat 9 vegetation indices were also closely aligned with the leaf spectrometer vegetation indices. The GNDVI and NDVI figures revealed that Landsat 9 has a better agreement with the leaf spectrometer than the Sentinel 2 and Drone. The MCARI figure showed a different case that the Landsat 9 has a better agreement with a drone than Sentinel 2. This might be because the MCARI is a narrow band vegetation index and is difficult to capture well with Drone and Landsat 9. In general terms, the leaf spectrometer vegetation indices do not align well with the vegetation indices of satellite and drone vegetation indices. This is in part due to the differences in specific wavelengths used for calculating respective VIs as different satellites and the Buteo drone vary in their wavelength collection bands while the SpectraVue spectrophotometer collects continuous data throughout the 360-1100 nm spectrum.

The result of the current study is different from other similar studies (Ke et al., 2015; Mezera et al., 2021), which compared the performance of optical Sensor and satellite images vegetation indices and found a modest correlation between them. One of the strengths of this research is the frequency of measurement, which is better than the current study. However, Polivova (2021) pointed out that the optical sensor vegetation indices are highly variable compared to the vegetation indices of multispectral images. Bareth et al. (2016) also compare uncalibrated multispectral images vegetation index with the NDVI from the optical spectrometer. According to the study, no strong correlation was found between the spectrometer NDVI and the multispectral RGBVI.

The inter and intra-comparison of Sentinel 2 and Landsat 9 sensors against the Unmanned Aerial Vehicle (UAV) has been analyzed using the R^2, RMSE, and a correlation matrix (Figures 4.26-4.31). The scatter plot and the correlation matrix showed that Sentinel 2 vegetation indices showed a fair correlation with Buteo drone vegetation indices, while Landsat 9 didn't show any correlation with the drone. Another low correlation was also observed between Landsat 9 and Sentinel 2 vegetation indices. The R^2 and RMSE values for different vegetation indices (Table 4.1) showed that Sentinel 2 and Drone have a relatively better

agreement than Landsat 9. The NDVI, EVI, SAVI, and SIPI scatter plots showed a better agreement between Sentinel 2 and the Buteo drone.

Several studies (Bollas et al., 2021; Korhonen et al., 2017a; Sozzi et al., 2020) support the result of the current study that Sentinel 2 and UAV vegetation indices have a higher correlation compared to the Landsat. Korhonen et al. (2017b) also compare the performance of UAV and Sentinel 2 and found a Pearson correlation coefficient between 0.5 to 0.7, which correlates with the result of the current study.

The correlation between the soil physicochemical properties and the NDVI of Sentinel 2, Landsat 9, and Drone is also portrayed in Figure 4.31. It has been observed that the NDVI of the leaf spectrometer was negatively correlated with the soil nitrogen, phosphorous, and potassium concentration, while it showed a positive correlation with soil pH at the measured five sampling points. The NDVI of the Buteo drone, on the other hand, showed a positive correlation with soil potassium and phosphorus and a highly negative correlation with soil nitrogen and soil pH. The Sentinel 2 NDVI, on the hand, showed a negative correlation with soil potassium and phosphorous while it showed a positive correlation with soil nitrogen and no correlation with soil pH. The NDVI of Landsat 9 showed a positive correlation with soil potassium and phosphorus and a negative correlation with soil nitrogen and ph.

Similar studies reported a different trend in the correlations between NDVI and soil physicochemical properties. Li et al. (2018) indicated that the NDVI has a very low correlation with soil pH and a high correlation with soil organic matter. Munyati et al. (2020) and Tola et al. 2017) revealed that the NDVI has no significant correlations between NDVI and soil nitrogen, phosphorus, and potassium.

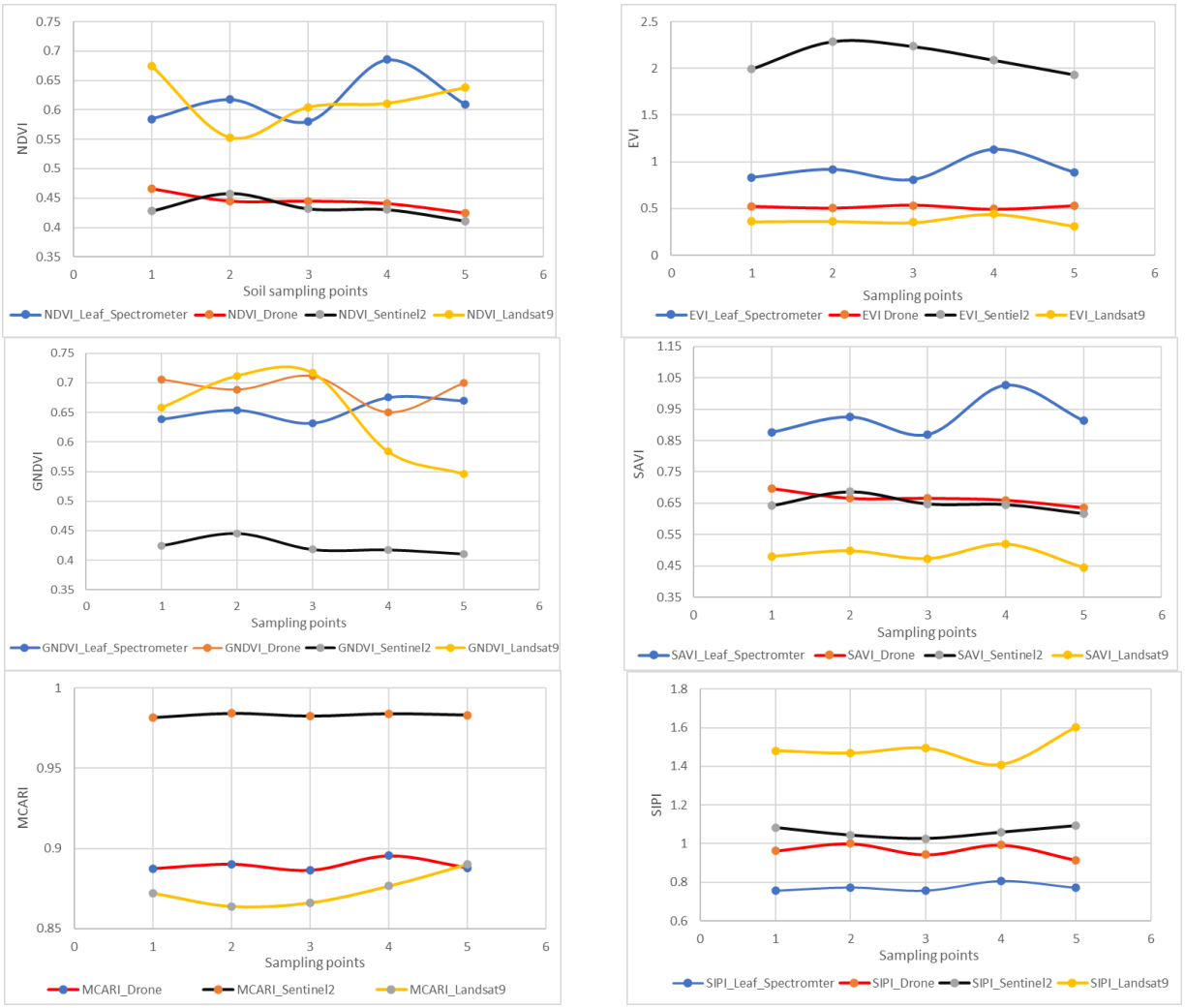

Figure 4.25. A comparison of Sentinel 2, Landsat 9, Buteo drone, and leaf spectrometer vegetation indices

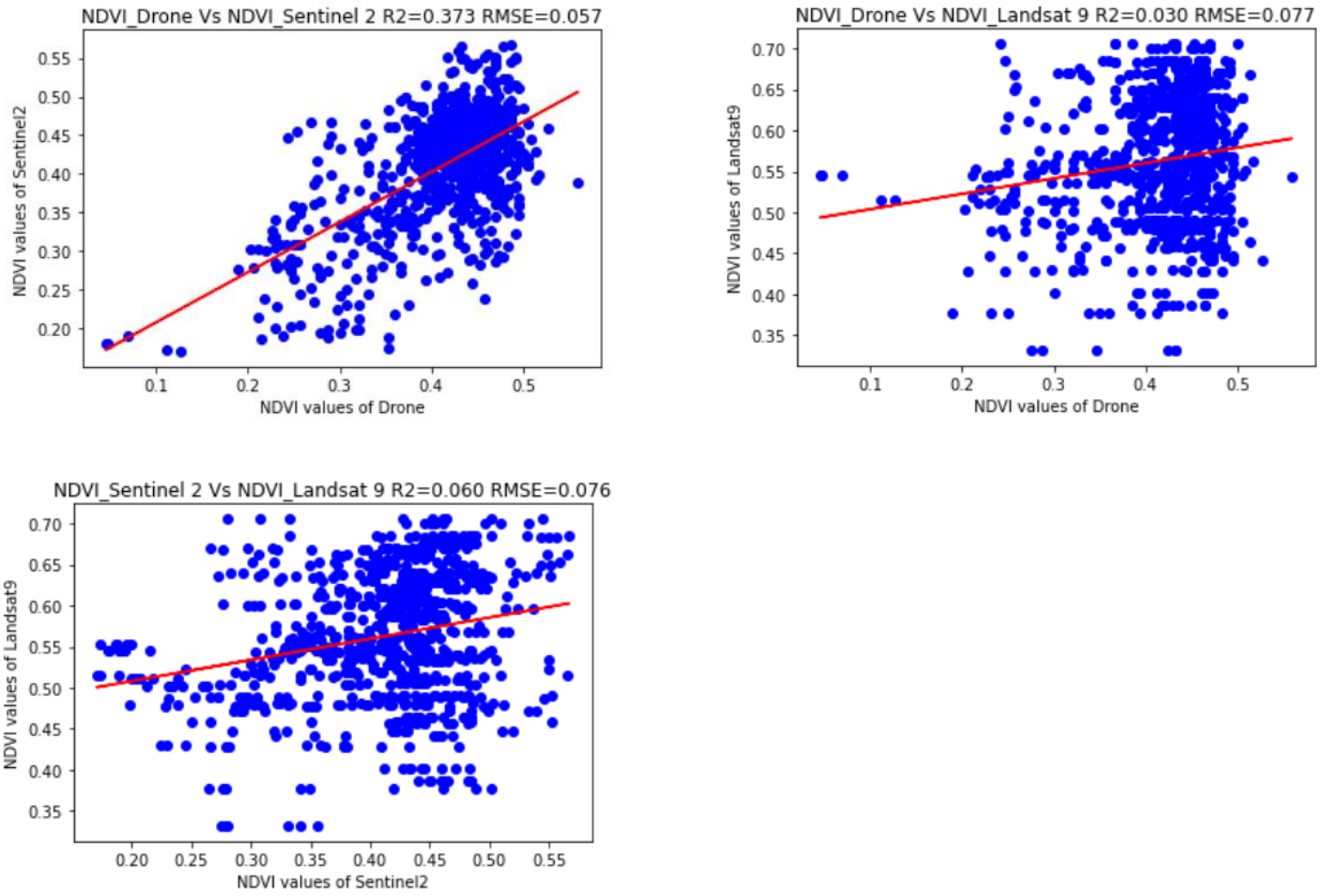

Figure 4.26. Scatter plot with its coefficient of determination and root mean square error of the Sentinel 2, Landsat 9, and Buteo drone vegetation indices against the Leaf Spectrometer vegetation indices

Table 4. 1. The coefficient of determination (R2) and root mean square error (RMSE) for the comparison of Sentinel 2, Landsat 9 and Bueto drone vegetation indices

Vegetation Indices	R^2 values			RMSE		
	Sentinel 2 Vs Drone	Landsat 9 Vs Drone	Sentinel 2 Vs Landsat 9	Sentinel 2 Vs Drone	Landsat 9 Vs Drone	Sentinel 2 Vs Landsat 9
NDVI	0.373	0.030	0.060	0.057	0.077	0.076
EVI	0.141	0.050	0.070	0.438	0.052	0.051
GNDVI	0.072	0.002	0.013	0.054	0.082	0.081
MCARI	0.014	0.002	0.013	0.004	0.082	0.081
SAVI	0.100	0.010	0.056	0.104	0.053	0.052
SIPI	0.330	0.051	0.052	0.106	0.141	0.141
CHLG	0.062	0.001	0.05	0.354	1.03	1.00
SR	0.001	0.000	0.043	0.130	0.850	0.832

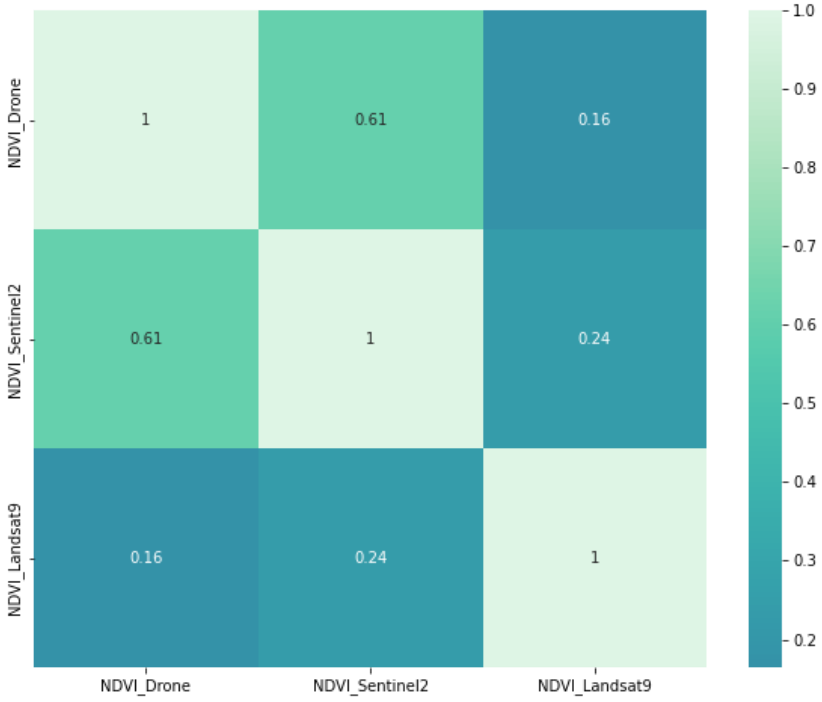

Figure 4.27. NDVI correlation matrix of the Sentinel 2, Landsat 9, Buteo drone, and Leaf Spectrometer

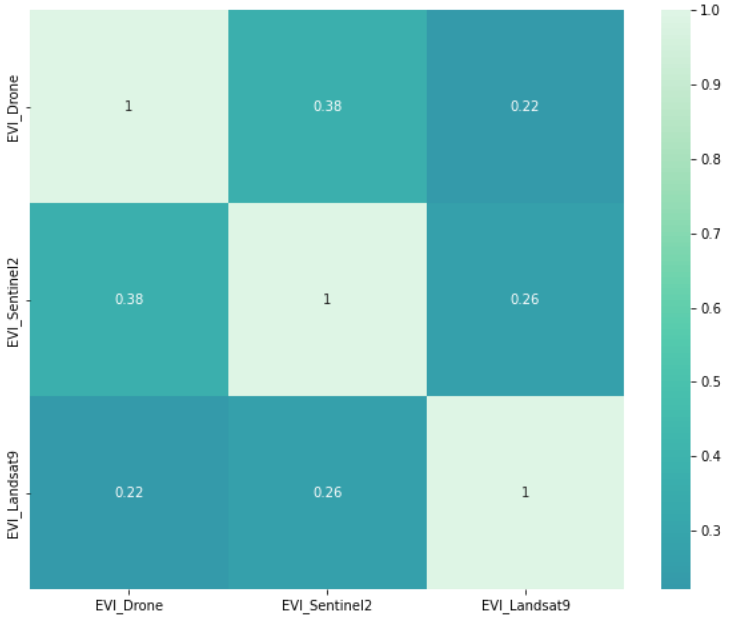

Figure 4.28. EVI correlation matrix of the Sentinel 2, Landsat 9, Buteo drone, and Leaf Spectrometer

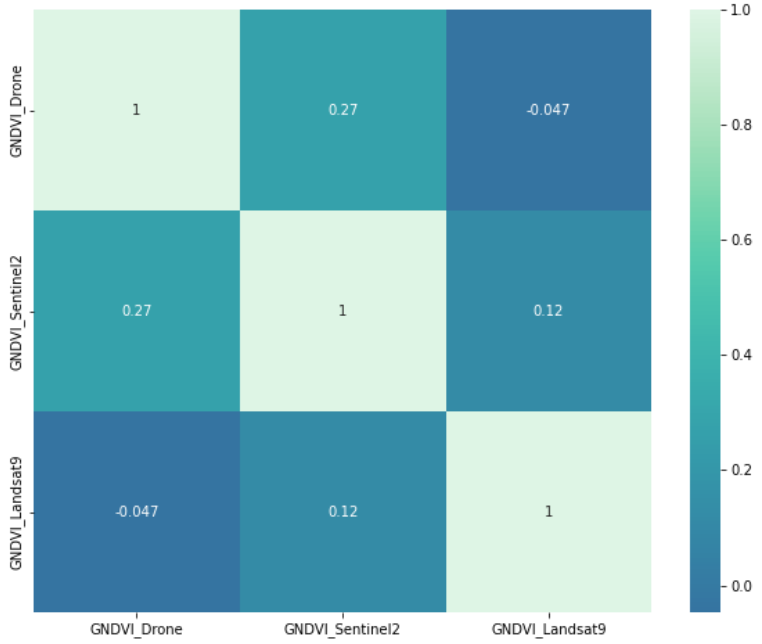

Figure 4.29. GNDVI correlation matrix of the Sentinel 2, Landsat 9, Buteo drone, and Leaf Spectrometer

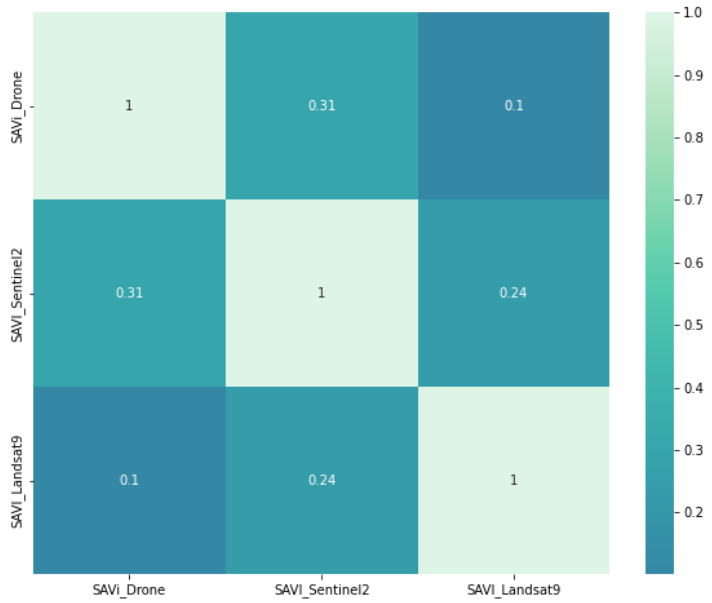

Figure 4.30. SAVI correlation matrix with a value of correlation coefficient of the Sentinel 2, Landsat 9, Buteo drone, and Leaf Spectrometer

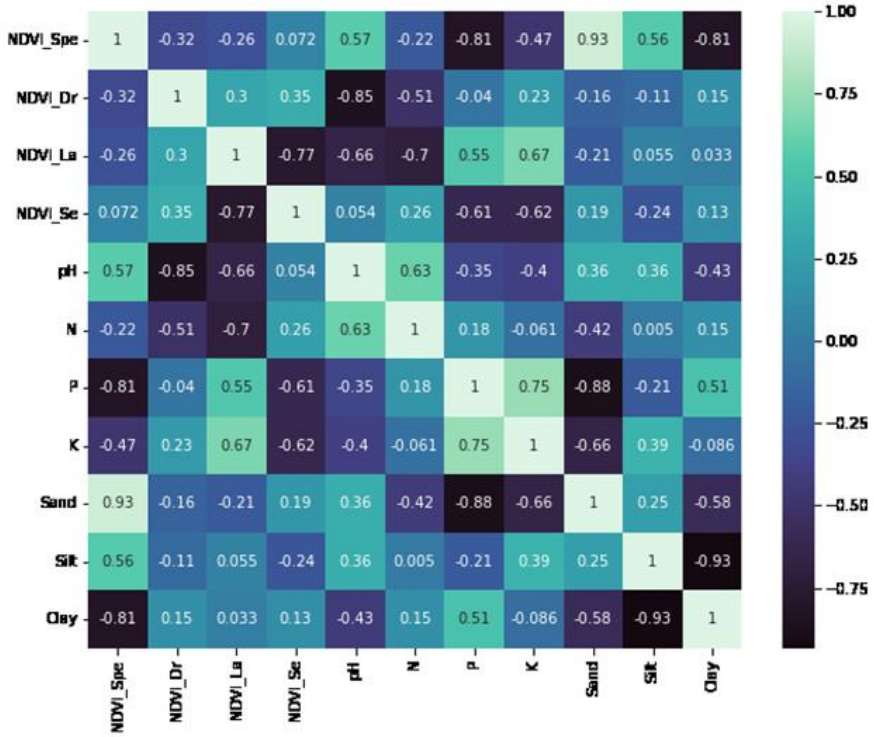

Figure 4.31. Correlation matrix between the soil physicochemical properties and NDVI of Sentinel 2, Buteo drone, and Landsat 9 and leaf spectrometer based on the measured five sampling points

5. CONCLUSIONS AND RECOMMENDATIONS

The current study assessed the potential performance of open data source satellite images (Sentinel 2 and Landsat 9) in estimating the biophysical properties of the wheat crop on a study farm found in the village of Ovcha Mogila. The finer resolution images from the UAV and the leaf spectral response measured using the SpectraVue CI-710s Leaf Spectrometer have been used to validate the satellite images. A soil sample has been collected at eight sampling points within the study farm to analyze its physicochemical properties.

The soil analysis showed that the study farm plot has a slightly alkaline pH. The study farm is dominated by Clay and Clay Loam soil texture. The maximum available nutrients (N, P, K) are concentrated in the Northeast part of the study area.

The results obtained also reveal that most of the values of vegetation indices are within the standard range and increased linearly with the growth of the plant. The Leaf Spectrometer does not capture the lower limits of most vegetation indices due to the fact that it measures only plant responses (without the background soil reflectance that other data collection approaches inevitably also include). Most of the values of the vegetation indices showed a consistency in which the maximum and the minimum values were mostly observed in the same part of the study area. The values of the vegetation indices are not at their uppermost possible range in early April, which indicates the crop has not reached peak growth.

The comparison vegetation indices of different sensors based on the five sampling points showed that Sentinel 2 and Drone have a better agreement over Landsat 9 and leaf spectrometer. In NDVI and GNDVI from the Landsat 9 showed a better agreement with the leaf spectrometer, while in MCARI, the Landsat 9 aligned better with the drone. A comparison of Sentinel 2 and Landsat 9 vegetation indices against the finer resolution drone image was performed using R^2, RMSE, and r. Both the scatter plot and the correlation matrix revealed that the Sentinel 2 vegetation indices have a better correlation with the drone than the Landsat 9. The highest correlation was observed between Sentinel 2 and drone, followed by Landsat 9 and Sentinel 2 vegetation indices. Generally, the Sentinel 2 VIs performed better than the Landsat 9 VIs.

Further study is required to further improve the quality of the current study. The number of leaf spectral response measurements and their frequency must be enough to represent the target farm area.

REFERENCES

Aguiar, D., Rudorff, B., Silva, W., Adami, M., & Mello, M. (2011). Remote Sensing Images in Support of Environmental Protocol: Monitoring the Sugarcane Harvest in SÃ£o Paulo State, Brazil. *Remote Sensing*, *3*, 2682–2703. https://doi.org/10.3390/rs3122682

Arvor, D., Jonathan, M., Simoes, M., Dubreuil, V., & Durieux, L. (2011). Classification of MODIS EVI time series for crop mapping in the state of Mato Grosso, Brazil. *International Journal of Remote Sensing*, *32*, 7847–7871. https://doi.org/10.1080/01431161.2010.531783

Bareth, G., Bolten, A., Gnyp, M. L., Reusch, S., & Jasper, J. (2016). COMPARISON OF UNCALIBRATED RGBVI WITH SPECTROMETER-BASED NDVI DERIVED FROM UAV SENSING SYSTEMS ON FIELD SCALE. *The International Archives of the Photogrammetry, Remote Sensing and Spatial Information Sciences*, *XLI-B8*, 837–843. https://doi.org/10.5194/isprs-archives-XLI-B8-837-2016

Bégué, A., Arvor, D., Lelong, C., Vintrou, E., Bégué, A., Arvor, D., Lelong, C., Vintrou, E., & Sys-, M. S. A. (2019). Agricultural Systems Studies using Remote Sensing To cite this version : HAL Id : hal-02098284. *Hal*.

Berger, M., Moreno, J., Johannessen, J. A., Levelt, P. F., & Hanssen, R. F. (2012). ESA's sentinel missions in support of Earth system science. *Remote Sensing of Environment*, *120*, 84–90.

Blackburn, G. A. (1998). Quantifying Chlorophylls and Caroteniods at Leaf and Canopy Scales: An Evaluation of Some Hyperspectral Approaches. *Remote Sensing of Environment*, *66*(3), 273–285. https://doi.org/https://doi.org/10.1016/S0034-4257(98)00059-5

Bollas, N., Kokinou, E., & Polychronos, V. (2021). Comparison of Sentinel-2 and UAV Multispectral Data for Use in Precision Agriculture: An Application from Northern Greece. In *Drones* (Vol. 5, Issue 2). https://doi.org/10.3390/drones5020035

Casanova, J. J., Judge, J., & Jones, J. W. (2006). Calibration of the CERES-Maize model for linkage with a microwave remote sensing model. *Transactions of the ASABE*, *49*(3), 783–792.

Cervantes-Godoy, D., Dewbre, J., Amegnaglo, C. J., Soglo, Y. Y., Akpa, A. F., Bickel, M., Sanyang, S., Ly, S., Kuiseu, J., Ama, S., Gautier, B. P., Officer, E. S., Officer, E. S., Eberlin, R., Officer, P., Branch, P. A., Oduro-ofori, E., Aboagye Anokye, P., Acquaye, N. E. A., … Swanson, B. E. (2014). The future of food and agriculture: trends and challenges. In *The future of food and agriculture: trends and challenges* (Vol. 4, Issue 4). www.fao.org/publications%0Ahttp://www.fao.org/3/a-i6583e.pdf%0Ahttp://siteresources.worldbank.org/INTARD/825826-1111044795683/20424536/Ag_ed_Africa.pdf%0Awww.fao.org/cfs%0Ahttp://www.jstor.org/stable/4356839%0Ahttps://ediss.uni-goettingen.de/bitstream/han

CID Bio-Science. (n.d.). *CID CI-710s.pdf*. https://www.cid-inc.com/plant-science-tools/leaf-spectroscopy/ci-710-miniature-leaf-spectrometer/

Colin, O., Hoersch, B., Marchese, F., Drusch, M., & Meygret, A. (2012). *OVERVIEW OF SENTINEL-2 European Space Agency , ESTEC , Noordwijk , Netherlands European Space Agency , ESRIN , Frascati , Italy European Space Agency , ESOC , Darmstadt , Germany Centre National d ' Etudes Spatiales , Toulouse , France*. *1*, 4–7.

Croft, H., Arabian, J., Chen, J. M., Shang, J., & Liu, J. (2020). Mapping within-field leaf chlorophyll content in agricultural crops for nitrogen management using Landsat-8 imagery. *Precision Agriculture*, *21*(4), 856–880. https://doi.org/10.1007/s11119-019-09698-y

Darnhofer, I., Bellon, S., Dedieu, B., & Milestad, R. (2010). Adaptiveness to enhance the sustainability of farming systems. A review. *Agronomy for Sustainable Development*, *30*(3), 545–555. https://doi.org/10.1051/agro/2009053

Darvishzadeh, R., Skidmore, A., Abdullah, H., Cherenet, E., Ali, A., Wang, T., Nieuwenhuis, W., Heurich, M., Vrieling, A., O'Connor, B., & Paganini, M. (2019). Mapping leaf chlorophyll content from Sentinel-2 and RapidEye data in spruce stands using the invertible forest reflectance model. *International Journal of Applied Earth Observation and Geoinformation*, *79*, 58–70. https://doi.org/https://doi.org/10.1016/j.jag.2019.03.003

Daughtry, C. S. T., Walthall, C. L., Kim, M. S., de Colstoun, E. B., & McMurtrey, J. E. (2000). Estimating Corn Leaf Chlorophyll Concentration from Leaf and Canopy Reflectance. *Remote Sensing of Environment*, *74*(2), 229–239. https://doi.org/https://doi.org/10.1016/S0034-4257(00)00113-9

Davis, E. (2018). *Comparison Of Sentinel-2 And Landsat 8 OLI In The Mapping Of Soil Salinity In Hyde County , North Carolina*. https://scholarcommons.sc.edu/etd/4870

Dimitrov, P., Filchev, L., Roumenina, E., & Jelev, G. (2021). *DOI : https://doi.org/10.3897/arb.v33.e04*. 40–50.

Drusch, M., Del Bello, U., Carlier, S., Colin, O., Fernandez, V., Gascon, F., Hoersch, B., Isola, C., Laberinti, P., & Martimort, P. (2012). Sentinel-2: ESA's optical high-resolution mission for GMES operational services. *Remote Sensing of Environment*, *120*, 25–36.

Ennouri, K., Smaoui, S., Gharbi, Y., Cheffi, M., Ben Braiek, O., Ennouri, M., & Triki, M. A. (2021). Usage of Artificial Intelligence and Remote Sensing as Efficient Devices to Increase Agricultural System Yields. *Journal of Food Quality*, *2021*. https://doi.org/10.1155/2021/6242288

Gao, B. (1996). NDWI—A normalized difference water index for remote sensing of vegetation liquid water from space. *Remote Sensing of Environment*, *58*(3), 257–266. https://doi.org/https://doi.org/10.1016/S0034-4257(96)00067-3

García-Llamas, P., Suárez-Seoane, S., Fernández-Guisuraga, J. M., Fernández-García, V., Fernández-Manso, A., Quintano, C., Taboada, A., Marcos, E., & Calvo, L. (2019). Evaluation and comparison of Landsat 8, Sentinel-2 and Deimos-1 remote sensing indices for assessing burn severity in Mediterranean fire-prone ecosystems. *International Journal of Applied Earth Observation and Geoinformation*, *80*(February 2019), 137–144. https://doi.org/10.1016/j.jag.2019.04.006

Gikov, A., Dimitrov, P., Filchev, L., Roumenina, E., & Jelev, G. (2019). Crop type mapping using multi-date imagery from the sentinel-2 satellites. *Comptes Rendus de L'Academie Bulgare Des Sciences*, *72*(6), 787–795. https://doi.org/10.7546/CRABS.2019.06.11

Gitelson, A. A., Kaufman, Y. J., & Merzlyak, M. N. (1996). Use of a green channel in remote sensing of global vegetation from EOS-MODIS. *Remote Sensing of Environment*, *58*(3), 289–298. https://doi.org/https://doi.org/10.1016/S0034-4257(96)00072-7

Gitelson, A. A., Merzlyak, M. N., & Chivkunova, O. B. (2001). Optical properties and non-destructive estimation of anthocyanin content in plant leaves. *Photochemistry and Photobiology*, *74*(1), 38–45. https://doi.org/10.1562/0031-8655(2001)074<0038:opaneo>2.0.co;2

Gitelson, A., Gritz, Y., & Merzlyak, M. (2003). Relationships between leaf chlorophyll content and spectral reflectance and algorithms for non-destructive chlorophyll assessment in higher plant leaves. *Journal of Plant Physiology*, *160*(3), 271–282. https://doi.org/https://doi.org/10.1078/0176-1617-00887

Gozdowski, D., Stępień, M., Panek, E., Varghese, J., Bodecka, E., Rozbicki, J., & Samborski, S. (2020). Comparison of winter wheat NDVI data derived from Landsat 8 and active

optical sensor at field scale. *Remote Sensing Applications: Society and Environment*, *20*, 100409. https://doi.org/https://doi.org/10.1016/j.rsase.2020.100409

Hansen, M. C., & Loveland, T. R. (2012). A review of large area monitoring of land cover change using Landsat data. *Remote Sensing of Environment*, *122*, 66–74. https://doi.org/https://doi.org/10.1016/j.rse.2011.08.024

Huete, A., Didan, K., Miura, T., Rodriguez, E. P., Gao, X., & Ferreira, L. G. (2002). Overview of the radiometric and biophysical performance of the MODIS vegetation indices. *Remote Sensing of Environment*, *83*(1), 195–213. https://doi.org/https://doi.org/10.1016/S0034-4257(02)00096-2

Huete, A. R. (1988). A soil-adjusted vegetation index (SAVI). *Remote Sensing of Environment*, *25*(3), 295–309. https://doi.org/https://doi.org/10.1016/0034-4257(88)90106-X

Kamenova, I., & Dimitrov, P. (2021). Evaluation of Sentinel-2 vegetation indices for prediction of LAI, fAPAR and fCover of winter wheat in Bulgaria. *European Journal of Remote Sensing*, *54*(sup1), 89–108. https://doi.org/10.1080/22797254.2020.1839359

Ke, Y., Im, J., Lee, J., Gong, H., & Ryu, Y. (2015). Characteristics of Landsat 8 OLI-derived NDVI by comparison with multiple satellite sensors and in-situ observations. *Remote Sensing of Environment*, *164*, 298–313. https://doi.org/https://doi.org/10.1016/j.rse.2015.04.004

Khanal, S., Kushal, K. C., Fulton, J. P., Shearer, S., & Ozkan, E. (2020). Remote sensing in agriculture—accomplishments, limitations, and opportunities. *Remote Sensing*, *12*(22), 1–29. https://doi.org/10.3390/rs12223783

Kingra, P. K., Majumder, D., & Singh, S. P. (2016). Application of Remote Sensing and Gis in Agriculture and Natural Resource Management Under Changing Climatic Conditions. *Agricultural Research Journal*, *53*(3), 295. https://doi.org/10.5958/2395-146x.2016.00058.2

Kolev, N., & Kozelov, L. (2015). Combined remote sensing and GIS technologies for land resources management in Bulgaria. *Bulgarian Journal of Agricultural Science*, *21*(4), 761–766.

Korhonen, L., Hadi, Packalen, P., & Rautiainen, M. (2017a). Comparison of Sentinel-2 and Landsat 8 in the estimation of boreal forest canopy cover and leaf area index. *Remote Sensing of Environment*, *195*, 259–274. https://doi.org/10.1016/j.rse.2017.03.021

Korhonen, L., Hadi, Packalen, P., & Rautiainen, M. (2017b). Comparison of Sentinel-2 and Landsat 8 in the estimation of boreal forest canopy cover and leaf area index. *Remote Sensing of Environment*, *195*, 259–274. https://doi.org/https://doi.org/10.1016/j.rse.2017.03.021

Léna Maatoug, Damien Arvor, Margareth Simões, A. B. (2012). Monitoring crop phenology in Mato Grosso (Brazil) using remote sensing data. *Paper Knowledge . Toward a Media History of Documents*.

Li, L., Zhang, Q., & Huang, D. (2014). A review of imaging techniques for plant phenotyping. *Sensors (Basel, Switzerland)*, *14*(11), 20078–20111. https://doi.org/10.3390/s141120078

Li, X., Yu, M., ma, J., Luo, Z., Chen, F., & Yang, Y. (2018). Identifying the Relationship between Soil Properties and Rice Growth for Improving Consolidated Land in the Yangtze River Delta, China. *Sustainability*, *10*, 3072. https://doi.org/10.3390/su10093072

Liaghat, S., & Balasundram, S. K. (2010). A review: The role of remote sensing in precision agriculture. *American Journal of Agricultural and Biological Science*, *5*(1), 50–55.

https://doi.org/10.3844/ajabssp.2010.50.55

Lorenzen, B., & Jensen, A. (1989). Changes in leaf spectral properties induced in barley by cereal powdery mildew. *Remote Sensing of Environment*, *27*(2), 201–209.

MacArthur, A., MacLellan, C., & Malthus, T. (2012). The Fields of View and Directional Response Functions of Two Field Spectroradiometers. *Geoscience and Remote Sensing, IEEE Transactions On*, *50*, 3892–3907. https://doi.org/10.1109/TGRS.2012.2185055

Malenovský, Z., Rott, H., Cihlar, J., Schaepman, M. E., García-Santos, G., Fernandes, R., & Berger, M. (2012). Sentinels for science: Potential of Sentinel-1,-2, and-3 missions for scientific observations of ocean, cryosphere, and land. *Remote Sensing of Environment*, *120*, 91–101.

Mashonganyika, F., Mugiyo, H., Svotwa, E., & Kutywayo, D. (2021). Mapping of Winter Wheat Using Sentinel-2 NDVI Data. A Case of Mashonaland Central Province in Zimbabwe . In *Frontiers in Climate* (Vol. 3). https://www.frontiersin.org/article/10.3389/fclim.2021.715837

Mezera, J., Lukas, V., Horniaček, I., Smutný, V., & Elbl, J. (2021). Comparison of Proximal and Remote Sensing for the Diagnosis of Crop Status in Site-Specific Crop Management. *Sensors (Basel, Switzerland)*, *22*(1), 19. https://doi.org/10.3390/s22010019

Miao, Y., Mulla, D. J., Randall, G. W., Vetsch, J. A., & Vintila, R. (2009). Combining chlorophyll meter readings and high spatial resolution remote sensing images for in-season site-specific nitrogen management of corn. *Precision Agriculture*, *10*(1), 45–62.

Moussaid, A., Fkihi, S. El, & Zennayi, Y. (2021). *Citrus Orchards Monitoring based on Remote Sensing and Artificial Intelligence Techniques: A Review of the Literature*. 172–178. https://doi.org/10.5220/0010432001720178

Munyati, C., Balzter, H., & Economon, E. (2020). Correlating Sentinel-2 MSI-derived vegetation indices with in-situ reflectance and tissue macronutrients in savannah grass. *International Journal of Remote Sensing*, *41*(10), 3820–3844. https://doi.org/10.1080/01431161.2019.1708505

Ndlovu, H. S., Odindi, J., Sibanda, M., Mutanga, O., Clulow, A., Chimonyo, V. G. P., & Mabhaudhi, T. (2021). A comparative estimation of maize leaf water content using machine learning techniques and unmanned aerial vehicle (Uav)-based proximal and remotely sensed data. *Remote Sensing*, *13*(20). https://doi.org/10.3390/rs13204091

Nellis. (1986). Nellis. *Applied Geography Conferences Vol. 9*, 56–62.

Nellis, M. D., Price, K. P., & Rundquist, D. (2009). Remote Sensing of Cropland Agriculture. *The SAGE Handbook of Remote Sensing*, 368–383. https://doi.org/10.4135/9780857021052.n26

Oza, S. R., Panigrahy, S., & Parihar, J. S. (2008). Concurrent use of active and passive microwave remote sensing data for monitoring of rice crop. *International Journal of Applied Earth Observation and Geoinformation*, *10*(3), 296–304. https://doi.org/10.1016/j.jag.2007.12.002

Ozdogan, M. (2010). The spatial distribution of crop types from MODIS data: Temporal unmixing using Independent Component Analysis. *Remote Sensing of Environment*, *114*, 1190–1204. https://doi.org/10.1016/j.rse.2010.01.006

Penuelas, J., Filella, I., Lloret, P., Munoz, F., & Vilajeliu, M. (1995). Reflectance assessment of mite effects on apple trees. *International Journal of Remote Sensing*, *16*(14), 2727–2733. https://doi.org/10.1080/01431169508954588

Polivova, M. (2021). *Detailed Investigation of Spectral Vegetation Indices for Fine Field-Scale Phenotyping* (A. B. E.-E. C. C. E.-A. C. O. E.-R. Q. C. E.-C. M. Musarella (ed.);

p. Ch. 7). IntechOpen. https://doi.org/10.5772/intechopen.96882

Price, K. P., Egbert, S. L., Nellis, M. D., Lee, R.-Y., & Boyce, R. (1997). Mapping Land Cover in a High Plains Agro-Ecosystem Using a Multidate Landsat Thematic Mapper Modeling Approach. *Transactions of the Kansas Academy of Science (1903-)*, *100*(1/2), 21–33. https://doi.org/10.2307/3628436

Ray, A. S. (2016). Remote Sensing in Agriculture Related papers Remote Sensing in Agriculture. *International Journal of Environment, Agriculture and Biotechnology (IJEAB)*, *1*(3), 362–367.

Sayler, K., & Zanter, K. (2022). Landsat 8 Level 2 Science Product (L2SP) Guide. *Nasa*, *2*(May), 1–43. https://prd-wret.s3.us-west-2.amazonaws.com/assets/palladium/production/atoms/files/LSDS-1619_Landsat8-C2-L2-ScienceProductGuide-v2.pdf

Shanmugapriya, P., Rathika, S., Ramesh, T., & Janaki, P. (2019). Applications of Remote Sensing in Agriculture - A Review. *International Journal of Current Microbiology and Applied Sciences*, *8*(01), 2270–2283. https://doi.org/10.20546/ijcmas.2019.801.238

Sozzi, M., Kayad, A., Marinello, F., Taylor, J., & Tisseyre, B. (2020). Comparing vineyard imagery acquired from Sentinel-2 and Unmanned Aerial Vehicle (UAV) platform. *OENO One*, *54*(2), 189–197. https://doi.org/10.20870/oeno-one.2020.54.1.2557

Stoyanov, A., Georgiev, N., Gigova, I., & Borisova, D. (2019). Application of remote sensing data for monitoring of forest vegetation on the territory of nature park “Blue Stones," Bulgaria. *Proc.SPIE*, *11149*. https://doi.org/10.1117/12.2538115

Sullivan, D. G., Strickland, T., & Masters, M. H. (2008). Satellite mapping of conservation tillage adoption in the Little River experimental watershed, Georgia. *Journal of Soil and Water Conservation*, *63*. https://doi.org/10.2489/63.3.112

Tenkorang, F., & Lowenberg-DeBoer, J. (2008). On-Farm Profitability of Remote Sensing in Agriculture. *Journal of Terrestrial Observation*, *1*(1), 6.

Thapa, S., Rudd, J. C., Xue, Q., Bhandari, M., Reddy, S. K., Jessup, K. E., Liu, S., Devkota, R. N., Baker, J., & Baker, S. (2019). Use of NDVI for characterizing winter wheat response to water stress in a semi-arid environment. *Journal of Crop Improvement*, *33*(5), 633–648. https://doi.org/10.1080/15427528.2019.1648348

Thenkabail, P., Enclona, E., Ashton, M., Van, B., & Meer, D. (2004). Accuracy assessments of hyperspectral waveband performance for vegetation analysis applications. *Remote Sensing of Environment - REMOTE SENS ENVIRON*, *91*. https://doi.org/10.1016/j.rse.2004.03.013

Thrall, P. H., Bever, J. D., & Burdon, J. J. (2010). Evolutionary change in agriculture: the past, present and future. *Evolutionary Applications*, *3*(5–6), 405–408. https://doi.org/10.1111/j.1752-4571.2010.00155.x

Tola, E., Al-Gaadi, K. A., Madugundu, R., Zeyada, A. M., Kayad, A. G., & Biradar, C. M. (2017). Characterization of spatial variability of soil physicochemical properties and its impact on Rhodes grass productivity. *Saudi Journal of Biological Sciences*, *24*(2), 421–429. https://doi.org/https://doi.org/10.1016/j.sjbs.2016.04.013

Ulfa, F., Orton, T. G., Dang, Y. P., & Menzies, N. W. (2022). Developing and Testing Remote-Sensing Indices to Represent within-Field Variation of Wheat Yields: Assessment of the Variation Explained by Simple Models. In *Agronomy* (Vol. 12, Issue 2). https://doi.org/10.3390/agronomy12020384

USDA. (1987). USDA Textural Soil Classification. In *Soil Mechanics Level I Module 3 - USDA Textural Soil Classification* (pp. 1–53).

USGS. (2013). Landsat. In *Van Nostrand’s Scientific Encyclopedia*.

https://doi.org/10.1002/0471743984.vse9497

USGS. (2021). Landsat 9 fact sheet. In *www.nasa.gov*. http://www.nasa.gov/centers/glenn/pdf/84790main_fs03grc.pdf

Verma, R. R., Manjunath, B. L., Singh, N. P., Kumar, A., Asolkar, T., Chavan, V., Srivastava, T. K., & Singh, P. (2018). Soil mapping and delineation of management zones in the Western Ghats of coastal India. *Land Degradation and Development*, *29*(12), 4313–4322. https://doi.org/10.1002/ldr.3183

Walter, A., Liebisch, F., & Hund, A. (2015). Plant phenotyping: from bean weighing to image analysis. *Plant Methods*, *11*(1), 14. https://doi.org/10.1186/s13007-015-0056-8

Wasonga, D. O. (2021). *Doctoral Programme in Sustainable Use of Renewable Natural Resources* (Issue May).

West, J. S., Bravo, C., Oberti, R., Lemaire, D., Moshou, D., & McCartney, H. A. (2003). THE POTENTIAL OF OPTICAL CANOPY MEASUREMENT FOR TARGETED CONTROL OF FIELD CROP DISEASES. *Annual Review of Phytopathology*, *41*(1), 593–614. https://doi.org/10.1146/annurev.phyto.41.121702.103726

Wikipedia. (2022). *Ovcha Mogila*. https://bg.wikipedia.org/wiki/Овча_могила

World Economic Forum, W. (2021). *Artificial Intelligence for Agriculture Domain.pdf*. *March*.

Xue, J., & Su, B. (2017). Significant Remote Sensing Vegetation Indices: A Review of Developments and Applications. *Journal of Sensors*, *2017*, 1353691. https://doi.org/10.1155/2017/1353691

Yang, I., & Acharya, T. D. (2015). Exploring Landsat 8. *International Journal of IT, Engineering and Applied Sciences Research*, *4*(4), 2319–4413. http://earthobservatory.nasa.gov/IOTD/

Yang, Y., Zhu, J., Zhao, C., Liu, S., & Tong, X. (2011). The spatial continuity study of NDVI based on Kriging and BPNN algorithm. *Mathematical and Computer Modelling*, *54*(3), 1138–1144. https://doi.org/https://doi.org/10.1016/j.mcm.2010.11.046

CURRICULUM VITA

Endalkachew Kebede has a BSc in Soil and Water Engineering and a MSc in Irrigation Engineering from Haramaya University, Ethiopia. He has more than eight years of experience as lecturer and researcher in different Ethiopian Universities. Endalkachew is a fellow of Erasmus Mundus Joint Master Degree in Soil Science under the consoritum of Ondokuz Mayis Universuty, University of Agriculture in Krakow and Agricultural University of Plovdiv.

Contact Information :

ORCID ID : 0000-0002-5212-7340

Publication

1. Endalkachew Kebede, Anadon V. Andonov , Bojin Bojinov, Orhan Dengiz (2021). Artificial intelligence and remote sensing as a tool for sustainable agriculture: A review. International Soil Science Symposium on “Soil Science & Plant Nutrition” 18 – 19 December 2021 / Samsun, Turkey. http://www.fesss.org/pages.php?id=6

2. Abebe, E. and Kebede, A. (2019). A Comparison of Hydrological Models Under Climate Change on the water resources of Megch River Catchment, Abbay Basin, Ethiopia, 2019. Journal of Natural science Research, 9.1.DOI: 10.7176/JNSR

3. Abebe, E. (2019). Grey water Irrigation: An Alternative Approach for Household Production, Journal of Civil and Environmental Research, Vol.11, No.2, 2019, DOI: 10.7176/CER

4. Abebe, E. and Kebede, A. (2017). Assessment of Climate Change Impacts on the Water Resources of Megech River Catchment, Abbay Basin, Ethiopia. Open Journal of Modern Hydrology,7, 141-152.

Won Awards, Incentives and Scholarships

1. Erasmus Mundus scholarship to study Erasmus Mundus Joint Master Degree in Soil Science at Ondokuz Mayis University, University of Agriculture in Krakow and Agricultural University of Plovdiv.